

Study of $B_{u,d,s} \rightarrow K_0^*(1430)P$ and $K_0^*(1430)V$ decays within QCD factorization

Lili Chen^a, Mengfei Zhao^a, Yunyun Zhang^{a,b} and Qin Chang^a

^aInstitute of Particle and Nuclear Physics, Henan Normal University, Henan 453007, China

^bNanyang Institute of Technology, Henan 473004, China

Abstract

We study the nonleptonic charmless $B_{u,d,s} \rightarrow K_0^*(1430)P$ ($P = K, \pi$) and $K_0^*(1430)V$ ($V = K^*, \rho, \omega, \phi$) decays. The amplitudes are calculated within the QCD factorization, and the non-perturbative quantities are evaluated by using a covariant light-front approach. The branching fractions and CP asymmetries of these decay modes are calculated, some decay modes are first predicted, and some useful relations based on $SU(3)$ flavor symmetry are discussed. Comparing the theoretical results with the current available experimental data, it is found that $K_0^*(1430)$ can be described as the lowest-lying p-wave ($s, u/d$) state rather than the first excited one.

1 Introduction

The inner structure of scalar (S) meson has been studied for a long time, and now it is still a hot topic in particle physics. There are several proposals for their inner structure, e.g., $\bar{q}q$ state, tetra-quark states, molecule states, glueball and hybrid states, while there is still no general agreement on such issue. For the light scalar mesons, in the 2-quark scenario (namely S1), it is suggested that the scalar mesons with mass below 1 GeV (such as $a_0(980)$, $f_0(980)$, $\kappa/K_0^*(700)$, etc.) are interpreted as the lowest lying $q\bar{q}$ states having a unit of orbital angular momentum and form a $SU(3)$ nonet; while, the ones with mass above 1 GeV (such as $a_0(1450)$, $f_0(1370)$, $K_0^*(1430)$, etc.) are treated as the first excited $q\bar{q}$ states and are classified into another $SU(3)$ nonet. On the contrary, in the tetra-quark scenario advocated by Jaffe [1, 2], the former are predominately the $qq\bar{q}\bar{q}$ states without introducing a unit of orbital angular momentum; accordingly, the later are treated as the lowest lying $q\bar{q}$ p-wave states (namely S2). This scenario is favored by some lattice calculations [3, 4] and mesonic spectroscopy data [5]; it is also much more acceptable because the 0^+ meson has a unit of orbital angular momentum and hence should have a higher mass above 1 GeV in the $q\bar{q}$ model. Besides of studies of mass spectra and decays of scalar mesons, the nonleptonic two-body B meson decay involving a scalar final state, $B \rightarrow SM$, provides another efficient way to investigate the features and the possible inner structures of scalar mesons.

In recent years, although the identification of scalar mesons is difficult experimentally, some experimental efforts have been devoted to measuring $B_{u,d} \rightarrow SM$ decay modes. For instance, the light scalar $f_0(980)$ was first observed in the $B \rightarrow f_0(980)K$ decay by the Belle [6] and BABAR [7] collaborations in 2002 and 2004, respectively. Since then, more and more $B \rightarrow SM$ decay modes have been observed by Belle [8–11], BABAR [12–20] and LHCb [21, 22] collaborations. Motivated by the rapid development of experiment, some theoretical studies on these decays are made within some QCD inspired approaches, such as the generalized factorization approach [23], QCD factorization (QCDF) [24–34], perturbative QCD approach (PQCD) [35–54] and other methods [55–66]. Most of these previous works mainly focus on the $B_{u,d} \rightarrow SM$ decay modes, but the $B_s \rightarrow SM$ decays have not been fully studied theoretically because most of the $B_s \rightarrow SM$ decay modes have not been observed.

In 2019, the $B_s \rightarrow K_0^*(1430)^+K^- + c.c.$ and $B_s \rightarrow \bar{K}_0^*(1430)^0K^0 + c.c.$ decays are observed

for the first time by LHCb collaboration, each with significance over 10 standard deviations. The measured branching fractions are [21]

$$\begin{aligned}\mathcal{B}(B_s^0 \rightarrow K_0^*(1430)^+ K^- + c.c.) &= (31.3 \pm 2.3 \pm 0.7 \pm 25.1 \pm 3.3) \times 10^{-6}, \\ \mathcal{B}(B_s^0 \rightarrow \bar{K}_0^*(1430)^0 K^0 + c.c.) &= (33.0 \pm 2.5 \pm 0.9 \pm 9.1 \pm 3.5) \times 10^{-6},\end{aligned}\quad (1)$$

Unfortunately, there is no relevant theoretical prediction for these decays before. It is expected that more $B_s \rightarrow SM$ decays will be observed by LHCb and Belle-II collaborations in the near future. Therefore, we would like to make a detailed study of $B_s \rightarrow K_0^*(1430)P$ and $K_0^*(1430)V$ (P denotes pseudoscalar meson, and V denotes vector meson) decay modes within the framework of QCDF in this paper. Besides, the $B_{u,d} \rightarrow K_0^*(1430)P$ and $K_0^*(1430)V$ decays will also be investigated¹. In order to test whether $K_0^*(1430)$ is a lowest lying $q\bar{q}$ state or a first excited state, our calculation and analysis will be made within the just mentioned two scenarios (S1 and S2).

This paper is organized as follows. In section 2, we present the theoretical framework and calculations for $B_{u,d,s} \rightarrow K_0^*(1430)P$, $K_0^*(1430)V$ decays. In section 3, the values of nonperturbative input parameters are calculated; after that, the numerical results and discussions are presented. Finally, we give our summary in section 4. The definitions of decay constant, form factor and distribution amplitude are given in appendix A, and the amplitudes of $B_{u,d,s} \rightarrow K_0^*(1430)P$, $K_0^*(1430)V$ decays are summarized in appendix B.

2 Theoretical framework

In the Standard Model (SM), the effective weak Hamiltonian responsible for $B_{u,d,s} \rightarrow M_1 M_2$ decay induced by $b \rightarrow p$ transition is given as [67]

$$\begin{aligned}\mathcal{H}_{\text{eff}} &= \frac{G_F}{\sqrt{2}} \left[V_{ub} V_{up}^* (C_1 O_1^u + C_2 O_2^u) + V_{cb} V_{cp}^* (C_1 O_1^c + C_2 O_2^c) \right. \\ &\quad \left. - V_{tb} V_{tp}^* \left(\sum_{i=3}^{10} C_i O_i + C_{7\gamma} O_{7\gamma} + C_{8g} O_{8g} \right) \right] + \text{h.c.},\end{aligned}\quad (2)$$

¹The $B_{u,d} \rightarrow SP$ and SV decay modes have been investigated in detail in Ref. [30] and Ref. [31], respectively. Some problems in these works are corrected and the predictions are updated by the same authors in Ref. [33]. Besides the corrections made in Ref. [33], some essential improvements will be made in this work.

where $V_{qb}V_{qp}^*$ ($q = u, c$ and t) are products of the Cabibbo-Kobayashi-Maskawa (CKM) matrix elements, C_i the Wilson coefficients, and O_i the relevant effective four-quark operators. To obtain the decay amplitude, the main work is to calculate the hadronic matrix element, $\langle M_1 M_2 | O_i | B \rangle$. In the QCDF, the hadronic matrix element of each operator can be written as the convolution integrals of the scattering kernel with the distribution amplitudes (DAs) of the participating mesons [68–70],

$$\begin{aligned} \langle M_1 M_2 | Q_i | B \rangle = & \sum_j F_j^{B \rightarrow M_1} f_{M_2} \int dy \mathcal{T}_{ij}^I(y) \varphi_{M_2}(y) + [M_1 \leftrightarrow M_2] \\ & + f_B f_{M_1} f_{M_2} \int dx dy dz \mathcal{T}_i^{II}(x, y, z) \varphi_{M_1}(x) \varphi_{M_2}(y) \varphi_B(z), \end{aligned} \quad (3)$$

where x, y, z are the momentum fractions; $F_j^{B \rightarrow M_1}$ is an appropriate form factor of $B \rightarrow M_1$ transition; f_B and f_M are decay constants of B and light mesons, respectively. The definitions of decay constant, form factor and DAs are given in the appendix A. The kernels $\mathcal{T}_{ij}^I(y)$ and $\mathcal{T}_i^{II}(x, y, z)$ in Eq. (3) are hard-scattering functions and are calculable in perturbation theory. The former starts at tree level and contains the vertex, penguin corrections at next-to-leading order in α_s ; the later contains the order α_s contributions caused by hard spectator-scattering and annihilation topologies.

Applying the factorization formula, one can obtain the amplitudes of $B_{u,d,s} \rightarrow K_0^*(1430)P$ and $K_0^*(1430)V$ decay modes, which are collected in the appendix B. In each amplitude, the quantity $A_{M_1 M_2}$ is the factorized matrix element and can be written as

$$A_{M_1 M_2} = \frac{G_F}{\sqrt{2}} \begin{cases} -(m_B^2 - m_{M_1}^2) U_0^{B \rightarrow M_1} (m_{M_2}^2) f_{M_2} & \text{if } M_1 M_2 = SP, \\ (m_B^2 - m_{M_1}^2) F_0^{B \rightarrow M_1} (m_{M_2}^2) f_{M_2} & \text{if } M_1 M_2 = PS, \\ 2m_{M_2} \epsilon^* \cdot p_B U_1^{B \rightarrow M_1} (m_{M_2}^2) f_{M_2} & \text{if } M_1 M_2 = SV, \\ -2m_{M_1} \epsilon^* \cdot p_B A_0^{B \rightarrow M_1} (m_{M_2}^2) f_{M_2} & \text{if } M_1 M_2 = VS. \end{cases} \quad (4)$$

Here, it has been assumed that the final-state meson M_1 carries away the spectator quark from B meson, and the other one is M_2 . The coefficients of flavor operators α_i^p appeared in the amplitudes are expressed in terms of the effective coefficients a_i^p as

$$\alpha_1(M_1 M_2) = a_1(M_1 M_2), \quad \alpha_2(M_1 M_2) = a_2(M_1 M_2), \quad (5)$$

$$\alpha_3^p(M_1 M_2) = \begin{cases} a_3^p(M_1 M_2) + a_5^p(M_1 M_2) & \text{if } M_1 M_2 = PS, SV, VS, \\ a_3^p(M_1 M_2) - a_5^p(M_1 M_2) & \text{if } M_1 M_2 = SP, \end{cases} \quad (6)$$

$$\alpha_4^p(M_1 M_2) = \begin{cases} a_4^p(M_1 M_2) - r_\chi^{M_2} a_6^p(M_1 M_2) & \text{if } M_1 M_2 = PS, SP, SV, \\ a_4^p(M_1 M_2) + r_\chi^{M_2} a_6^p(M_1 M_2) & \text{if } M_1 M_2 = VS, \end{cases} \quad (7)$$

$$\alpha_{3,EW}^p(M_1 M_2) = \begin{cases} a_9^p(M_1 M_2) + a_7^p(M_1 M_2) & \text{if } M_1 M_2 = PS, SV, VS, \\ a_9^p(M_1 M_2) - a_7^p(M_1 M_2) & \text{if } M_1 M_2 = SP, \end{cases} \quad (8)$$

$$\alpha_{4,EW}^p(M_1 M_2) = \begin{cases} a_{10}^p(M_1 M_2) - r_\chi^{M_2} a_8^p(M_1 M_2) & \text{if } M_1 M_2 = PS, SP, SV, \\ a_{10}^p(M_1 M_2) + r_\chi^{M_2} a_8^p(M_1 M_2) & \text{if } M_1 M_2 = VS, \end{cases} \quad (9)$$

where the ratio r_χ is defined as

$$r_\chi^P(\mu) = \frac{2m_P^2}{m_b(\mu)(m_1(\mu) + m_2(\mu))}, \quad r_\chi^V(\mu) = \frac{2m_V}{m_b(\mu)} \frac{f_V^\perp(\mu)}{f_V}, \quad (10)$$

$$r_\chi^S(\mu) = \frac{2m_S}{m_b(\mu)} \frac{\bar{f}_S(\mu)}{f_S} = \frac{2m_S^2}{m_b(\mu)(m_1(\mu) - m_2(\mu))}. \quad (11)$$

In Eqs. (5-9), the general form of effective coefficient a_i^p at next-to-leading order in α_s is

$$a_i^p(M_1 M_2) = \left(C_i + \frac{C_{i\pm 1}}{N_c} \right) N_i(M_2) + \frac{C_{i\pm 1}}{N_c} \frac{C_F \alpha_s}{4\pi} \left[V_i(M_2) + \frac{4\pi^2}{N_c} H_i(M_1 M_2) \right] + P_i^p(M_2), \quad (12)$$

where $i = 1, \dots, 10$, the upper (lower) sign applies when i is odd (even), $C_F = (N_c^2 - 1)/(2N_c)$ with $N_c = 3$, and $N_i(M_2) = 1$ except for $N_{6,8}(V) = 0$. The terms proportional to $N_i(M_2)$ are the leading order contributions, and are the same as the results obtained by naive factorization approach; the α_s corrections are encoded in the quantities $V_i(M_2)$, $H_i(M_1 M_2)$ and $P_i^p(M_2)$, which are obtained by calculating vertex, hard-spectator and penguin diagrams, and can be written as the convolution integrals of the hard-scattering kernels with meson light-cone DAs. The convolution integrals for these quantities can be evaluated by using expansions of the DAs in terms of Gegenbauer polynomials. In this work, we include the first four terms in the Gegenbauer expansion for the twist-2 DAs due to the nontrivial contribution related to the odd Gegenbauer moments of scalar meson.

The integral forms of $V_i(M_2)$ and $P_i^p(M_2)$ for $B \rightarrow SP$ and SV modes are the same as the ones for $B \rightarrow PP$ and PV modes, which have been obtained in Ref. [70]. After integrating out

the momentum fraction, we obtain

$$V_i(M_2) = (12 \ln \frac{m_b}{\mu} - \frac{37}{2} - 3i\pi)a_0^{M_2} + (\frac{11}{2} - 3i\pi)a_1^{M_2} - \frac{21}{20}a_2^{M_2} + (\frac{79}{36} - \frac{2i\pi}{3})a_3^{M_2} \quad (13)$$

for $i = 1 - 4, 9, 10$, and

$$V_i(M_2) = (-12 \ln \frac{m_b}{\mu} + \frac{13}{2} + 3i\pi)a_0^{M_2} + (\frac{11}{2} - 3i\pi)a_1^{M_2} + \frac{21}{20}a_2^{M_2} + (\frac{79}{36} - \frac{2i\pi}{3})a_3^{M_2} \quad (14)$$

for $i = 5, 7$ when $M_2 = P, S, V$; while, for $i = 6$ and 8 , we have

$$V_i(M) = \begin{cases} -6 & \text{if } M_2 = P \text{ and } S, \\ 9 - 6\pi i & \text{if } M_2 = V. \end{cases} \quad (15)$$

It is noted that our result given by Eq. (14) is different from the one given in Ref. [30] but is consistent with the one given by the same authors in Ref. [31]. For the penguin functions $G_{M_2}(s)$ appeared in $P_i^p(M_2)$ (one may refer to Ref. [70] for detail), we have the following analytic results,

$$G_{M_2}(0) = \left(\frac{5}{3} + \frac{2i\pi}{3}\right)a_0^{M_2} + \frac{a_1^{M_2}}{2} + \frac{a_2^{M_2}}{5} + \frac{a_3^{M_2}}{9}, \quad (16)$$

$$\begin{aligned} G_{M_2}(s_c) = & \left(\frac{5}{3} - \frac{2}{3} \ln s_c\right)a_0^{M_2} + \frac{a_1^{M_2}}{2} + \frac{a_2^{M_2}}{5} + \frac{a_3^{M_2}}{9} + \frac{4}{3} \left(8a_0^{M_2} + 9a_1^{M_2} + 9a_2^{M_2} + 9a_3^{M_2}\right) s_c \\ & + 2(8a_0^{M_2} + 63a_1^{M_2} + 214a_2^{M_2} + \frac{1505a_3^{M_2}}{3})s_c^2 - 24(9a_1^{M_2} + 80a_2^{M_2} + \frac{9490a_3^{M_2}}{27})s_c^3 \\ & + (2880a_2^{M_2} + \frac{91000a_3^{M_2}}{3})s_c^4 - 39200a_3^{M_2}s_c^5 - \frac{2}{3}\sqrt{1-4s_c} \left[(1+2s_c)a_0^{M_2} \right. \\ & + 6(4a_0^{M_2} + 27a_1^{M_2} + 78a_2^{M_2} + 160a_3^{M_2})s_c^2 - 36(9a_1^{M_2} + 70a_2^{M_2} + \frac{2440a_3^{M_2}}{9})s_c^3 \\ & \left. + (4320a_2^{M_2} + 40600a_3^{M_2})s_c^4 - 58800a_3^{M_2}s_c^5 \right] (2 \operatorname{arctanh} \sqrt{1-4s_c} - i\pi) + 12s_c^2 \left[a_0^{M_2} \right. \\ & + 3a_1^{M_2} + 6a_2^{M_2} + 10a_3^{M_2} - \frac{4}{3} \left(a_0^{M_2} + 9a_1^{M_2} + 36a_2^{M_2} + 100a_3^{M_2} \right) s_c + 18(a_1^{M_2} + 10a_2^{M_2} + 50a_3^{M_2})s_c^2 \\ & \left. - (240a_2^{M_2} + 2800a_3^{M_2})s_c^3 + \frac{9800a_3^{M_2}}{3}s_c^4 \right] (2 \operatorname{arctanh} \sqrt{1-4s_c} - i\pi)^2, \quad (17) \end{aligned}$$

$$\begin{aligned} G_{M_2}(1) = & \left(\frac{85}{3} - 6\sqrt{3}\pi + \frac{4\pi^2}{9}\right)a_0^{M_2} - \left(\frac{155}{2} - 36\sqrt{3}\pi + 12\pi^2\right)a_1^{M_2} \\ & + \left(\frac{7001}{5} - 504\sqrt{3}\pi + 136\pi^2\right)a_2^{M_2} - \left(\frac{146581}{9} - 6000\sqrt{3}\pi + \frac{14920}{9}\pi^2\right)a_3^{M_2}. \quad (18) \end{aligned}$$

where, $s_c = (m_c/m_b)^2$; while, the functions $\hat{G}_{M_2}(s)$ read

$$\hat{G}_{M_2}(s_c) = \frac{16}{9}(1-3s_c) - \frac{2}{3}\ln s_c - \frac{2}{3}(1-4s_c)^{3/2}(2 \operatorname{arctanh} \sqrt{1-4s_c} - i\pi),$$

$$\hat{G}_{M_2}(0) = \frac{16}{9} + \frac{2\pi}{3}i, \quad \hat{G}_{M_2}(1) = \frac{2\pi}{\sqrt{3}} - \frac{32}{9}, \quad (19)$$

when $M_2 = P, S$, and

$$\begin{aligned} \hat{G}_{M_2}(s_c) &= 1 - 36s_c + 12s_c\sqrt{1-4s_c}(2\arctanh\sqrt{1-4s_c} - i\pi) - 12s_c^2(2\arctanh\sqrt{1-4s_c} - i\pi)^2, \\ \hat{G}_{M_2}(0) &= 1, \quad \hat{G}_{M_2}(1) = -35 + 4\sqrt{3}\pi + \frac{4\pi^2}{3}, \end{aligned} \quad (20)$$

when $M_2 = V$.

The hard-spectator corrections can be written as

$$H_i(M_1M_2) = \frac{B_{M_1M_2}}{A_{M_1M_2}} \int_0^1 \frac{d\xi}{\xi} \Phi_B(\xi) \int_0^1 dx \int_0^1 dy \left[\frac{\Phi_{M_2}(x)\Phi_{M_1}(y)}{\bar{x}\bar{y}} \pm \gamma_\chi^{M_1} \frac{\Phi_{M_2}(x)\phi_{M_1}(y)}{x\bar{y}} \right] \quad (21)$$

for $i = 1 - 4, 9, 10$,

$$H_i(M_1M_2) = -\frac{B_{M_1M_2}}{A_{M_1M_2}} \int_0^1 \frac{d\xi}{\xi} \Phi_B(\xi) \int_0^1 dx \int_0^1 dy \left[\frac{\Phi_{M_2}(x)\Phi_{M_1}(y)}{x\bar{y}} \pm \gamma_\chi^{M_1} \frac{\Phi_{M_2}(x)\phi_{M_1}(y)}{\bar{x}\bar{y}} \right] \quad (22)$$

for $i = 5, 7$, and $H_i(M_1M_2) = 0$ for $i = 6, 8$, where $\bar{x} = 1 - x$, $\bar{y} = 1 - y$. The upper (lower) sign should be applied when $M_1 = V, P$ ($M_1 = S$). The quantity $B_{M_1M_2}$ is defined as

$$B_{M_1M_2} = \frac{G_F}{\sqrt{2}} \begin{cases} f_{B_q} f_{M_1} f_{M_2} & \text{if } M_1M_2 = PS, SP, \\ -f_{B_q} f_{M_1} f_{M_2} & \text{if } M_1M_2 = VS, SV. \end{cases} \quad (23)$$

Integrating out the momentum fraction, we can finally obtain

$$H_i = \frac{B_{M_1M_2}}{A_{M_1M_2}} \frac{m_B}{\lambda_B} \cdot \begin{cases} \left[3(a_0^{M_1} + a_1^{M_1} + a_2^{M_1} + a_3^{M_1}) \cdot 3(a_0^{M_2} + a_1^{M_2} + a_2^{M_2} + a_3^{M_2}) \right. \\ \quad \left. \pm 3\gamma_\chi^{M_1}(a_0^{M_2} - a_1^{M_2} + a_2^{M_2} - a_3^{M_2})X_H \right], & M_1 = P (S), \quad (24) \\ \left[3(a_0^{M_1} + a_1^{M_1} + a_2^{M_1} + a_3^{M_1}) \cdot 3(a_0^{M_2} + a_1^{M_2} + a_2^{M_2} + a_3^{M_2}) \right. \\ \quad \left. + 3\gamma_\chi^{M_1}(a_0^{M_2} - a_1^{M_2} + a_2^{M_2} - a_3^{M_2})(3X_H - 6) \right], & M_1 = V, \quad (25) \end{cases}$$

for $i = 1 - 4, 9, 10$, and

$$H_i = -\frac{B_{M_1M_2}}{A_{M_1M_2}} \frac{m_B}{\lambda_B} \cdot \begin{cases} \left[3(a_0^{M_1} + a_1^{M_1} + a_2^{M_1} + a_3^{M_1}) \cdot 3(a_0^{M_2} - a_1^{M_2} + a_2^{M_2} - a_3^{M_2}) \right. \\ \quad \left. \pm 3\gamma_\chi^{M_1}(a_0^{M_2} + a_1^{M_2} + a_2^{M_2} + a_3^{M_2})X_H \right], & M_1 = P (S), \quad (26) \\ \left[3(a_0^{M_1} + a_1^{M_1} + a_2^{M_1} + a_3^{M_1}) \cdot 3(a_0^{M_2} - a_1^{M_2} + a_2^{M_2} - a_3^{M_2}) \right. \\ \quad \left. + 3\gamma_\chi^{M_1}(a_0^{M_2} + a_1^{M_2} + a_2^{M_2} + a_3^{M_2})(3X_H - 6) \right], & M_1 = V, \quad (27) \end{cases}$$

for $i = 5$ and 7 , where, the upper (lower) sign in Eqs. (24) and (26) is applied when $M_1 = P (S)$. As has been discussed in many previous works [33, 56, 70–76], hard-spectator corrections suffer from the end-point divergence, which is usually parameterized by the end-point parameter

$$X_H = \ln \left(\frac{m_B}{\Lambda_h} \right) (1 + \rho_H e^{i\phi_H}). \quad (28)$$

The parameters ρ_H and ϕ_H reflect the strength and possible strong phase of the end-point contributions, respectively.

The amplitudes of $B_{u,d,s} \rightarrow K_0^*(1430)P$ and $K_0^*(1430)V$ decays collected in the appendix B also receives the contributions of weak annihilation, which are involved in the effective coefficients β_i^p defined as

$$\beta_i^p(M_1 M_2) \equiv \frac{B_{M_1 M_2}}{A_{M_1 M_2}} b_i^p, \quad (29)$$

where,²

$$\begin{aligned} b_1 &= \frac{C_F}{N_c^2} C_1 A_1^i, & b_2 &= \frac{C_F}{N_c^2} C_2 A_1^i, \\ b_3^p &= \frac{C_F}{N_c^2} [C_3 A_1^i + C_5 (A_3^i + A_3^f) + N_c C_6 A_3^f], & b_4^p &= \frac{C_F}{N_c^2} [C_4 A_1^i + C_6 A_2^i], \\ b_{3,EW}^p &= \frac{C_F}{N_c^2} [C_9 A_1^i + C_7 (A_3^i + A_3^f) + N_c C_8 A_3^f], & b_{4,EW}^p &= \frac{C_F}{N_c^2} [C_{10} A_1^i + C_8 A_2^i]. \end{aligned} \quad (30)$$

The subscripts $n = 1, 2, 3$ of $A_n^{i,f}$ correspond to the possible Dirac structures $(V - A)(V - A)$, $(V - A)(V + A)$ and $(S - P)(S + P)$, respectively; and the superscripts i and f refer to gluon emission from the initial- and final-state quarks, respectively. The explicit expressions of $A_n^{i,f}$ for $B \rightarrow PS$ and SP decays can be written as

$$A_1^i = \pi \alpha_s \int_0^1 dx dy \left\{ \Phi_{M_2}(x) \Phi_{M_1}(y) \left[\frac{1}{y(1-x\bar{y})} + \frac{1}{\bar{x}^2 y} \right] \mp \gamma_\chi^{M_1} \gamma_\chi^{M_2} \phi_{M_2}(x) \phi_{M_1}(y) \frac{2}{\bar{x}y} \right\}, \quad (31)$$

$$A_1^f = 0; \quad (32)$$

$$A_2^i = \pi \alpha_s \int_0^1 dx dy \left\{ -\Phi_{M_2}(x) \Phi_{M_1}(y) \left[\frac{1}{\bar{x}(1-x\bar{y})} + \frac{1}{\bar{x}y^2} \right] \pm \gamma_\chi^{M_1} \gamma_\chi^{M_2} \phi_{M_2}(x) \phi_{M_1}(y) \frac{2}{\bar{x}y} \right\}, \quad (33)$$

$$A_2^f = 0, \quad (34)$$

$$A_3^i = \pi \alpha_s \int_0^1 dx dy \left\{ \pm \gamma_\chi^{M_1} \Phi_{M_2}(x) \phi_{M_1}(y) \frac{2\bar{y}}{\bar{x}y(1-x\bar{y})} + \gamma_\chi^{M_2} \phi_{M_2}(x) \Phi_{M_1}(y) \frac{2x}{\bar{x}y(1-x\bar{y})} \right\}, \quad (35)$$

²In Refs. [30, 31], the superscript of the last terms in b_4^p and $b_{3,EW}^p$ (Eq. (3.12)) should be corrected, *i.e.*, $A_2^f \rightarrow A_2^i$ and $A_3^f \rightarrow A_3^f$.

$$A_3^f = \pi\alpha_s \int_0^1 dx dy \left\{ \pm \gamma_\chi^{M_1} \Phi_{M_2}(x) \phi_{M_1}(y) \frac{2(1+\bar{x})}{\bar{x}^2 y} - \gamma_\chi^{M_2} \phi_{M_2}(x) \Phi_{M_1}(y) \frac{2(1+y)}{\bar{x} y^2} \right\}, \quad (36)$$

where, the upper and lower signs are applied to $B \rightarrow PS$ and SP decays, respectively. The $A_n^{i,f}$ for $B \rightarrow VS$ decay can be obtained from the $A_n^{i,f}$ for $B \rightarrow PS$ decay by changing the sign of second term in $A_{1,3}^i$ and A_3^f , and the first term in A_2^i ; while, the $A_n^{i,f}$ for $B \rightarrow SV$ decay is the same as $A_n^{i,f}$ for $B \rightarrow SP$ decay except for the overall sign of A_2^i . After integrating out the momentum fractions, we can finally obtain

$$A_1^i(PS) \approx 2\pi\alpha_s \left\{ 9 \left[a_0^{M_2} (X_A - 4 + \frac{\pi^2}{3}) + a_1^{M_2} (3X_A + 4 - \pi^2) + a_2^{M_2} (6X_A - \frac{107}{3} + 2\pi^2) + a_3^{M_2} (10X_A + \frac{23}{18} - \frac{10}{3}\pi^2) \right] - \gamma_\chi^P \gamma_\chi^S X_A^2 \right\}, \quad (37)$$

$$A_2^i(PS) \approx 2\pi\alpha_s \left\{ -9 \left[a_0^{M_2} (X_A - 4 + \frac{\pi^2}{3}) + a_1^{M_2} (X_A + 29 - 3\pi^2) + a_2^{M_2} (X_A - 119 + 12\pi^2) + a_3^{M_2} (X_A + \frac{2956}{9} - \frac{100}{3}\pi^2) \right] + \gamma_\chi^P \gamma_\chi^S X_A^2 \right\}, \quad (38)$$

$$A_3^i(PS) \approx 6\pi\alpha_s \left\{ \gamma_\chi^P \left[a_0^{M_2} (X_A^2 - 2X_A + \frac{\pi^2}{3}) + 3a_1^{M_2} (X_A^2 - 4X_A + 4 + \frac{\pi^2}{3}) + 6a_2^{M_2} (X_A^2 - \frac{16}{3}X_A + \frac{15}{2} + \frac{\pi^2}{3}) + 10a_3^{M_2} (X_A^2 - \frac{19}{3}X_A + \frac{191}{18} + \frac{\pi^2}{3}) \right] + \gamma_\chi^S (X_A^2 - 2X_A + \frac{\pi^2}{3}) \right\}, \quad (39)$$

$$A_3^f(PS) \approx 6\pi\alpha_s X_A \left\{ \gamma_\chi^P \left[a_0^{M_2} (2X_A - 1) + a_1^{M_2} (6X_A - 11) + a_2^{M_2} (12X_A - 31) + a_3^{M_2} (20X_A - \frac{187}{3}) \right] - \gamma_\chi^S (2X_A - 1) \right\} \quad (40)$$

for $M_1 M_2 = PS$, and

$$A_1^i(VS) \approx 6\pi\alpha_s \left\{ 3 \left[a_0^{M_2} (X_A - 4 + \frac{\pi^2}{3}) + a_1^{M_2} (3X_A + 4 - \pi^2) + a_2^{M_2} (6X_A - \frac{107}{3} + 2\pi^2) + a_3^{M_2} (10X_A + \frac{23}{18} - \frac{10}{3}\pi^2) \right] - \gamma_\chi^V \gamma_\chi^S X_A (X_A - 2) \right\}, \quad (41)$$

$$A_2^i(VS) \approx 6\pi\alpha_s \left\{ 3 \left[a_0^{M_2} (X_A - 4 + \frac{\pi^2}{3}) + a_1^{M_2} (X_A + 29 - 3\pi^2) + a_2^{M_2} (X_A - 119 + 12\pi^2) + a_3^{M_2} (X_A + \frac{2956}{9} - \frac{100}{3}\pi^2) \right] - \gamma_\chi^V \gamma_\chi^S X_A (X_A - 2) \right\}, \quad (42)$$

$$A_3^i(VS) \approx 6\pi\alpha_s \left\{ -\gamma_\chi^V \left[3a_0^{M_2} (X_A^2 - 2X_A + 4 - \frac{\pi^2}{3}) + 9a_1^{M_2} (X_A^2 - 4X_A - 4 + \pi^2) + 3a_2^{M_2} (6X_A^2 - 32X_A + 79 - 2\pi^2) + 10a_3^{M_2} (3X_A^2 - 19X_A + \frac{61}{6} + 3\pi^2) \right] \right\}$$

$$- \gamma_\chi^S \left(X_A^2 - 2X_A + \frac{\pi^2}{3} \right) \Big\}, \quad (43)$$

$$A_3^f(VS) \approx 6\pi\alpha_s \left\{ -3\gamma_\chi^V (X_A - 2) \left[a_0^{M_2} (2X_A - 1) + a_1^{M_2} (6X_A - 11) + a_2^{M_2} (12X_A - 31) \right. \right. \\ \left. \left. + a_3^{M_2} \left(20X_A - \frac{187}{3} \right) \right] + \gamma_\chi^S X_A (2X_A - 1) \right\} \quad (44)$$

for $M_1 M_2 = VS$, where, X_A is the endpoint parameter and is defined in the same manner as X_H given by Eq. (28). The results for the cases of $M_1 M_2 = SP$ and $M_1 M_2 = SV$ can be obtained via the relation

$$A_1^i(SP) = A_2^i(PV), \quad A_2^i(SP) = A_1^i(PV), \quad A_3^i(SP) = -A_3^i(PV), \quad A_3^f(SP) = A_3^f(PV), \quad (45)$$

$$A_1^i(SV) = -A_2^i(VS), \quad A_2^i(SV) = -A_1^i(VS), \quad A_3^i(SV) = A_3^i(VS), \quad A_3^f(SV) = -A_3^f(VS), \quad (46)$$

but with different sign of $a_0^{M_2}$ and $a_2^{M_2}$. In above evaluation, the asymptotic DAs of P and V mesons are used for simplicity; while, for the DA of S meson, the first four terms in Gegenbauer expansion are included because of the dominance of a_1^S . In the previous works [30–33], the contributions related to a_0^S and a_2^S are neglected, which is reasonable for the cases of scalar (u, d) state and quarkonium because $a_{0,2}^S \simeq 0$. However, for the case of $K_0^*(1430)$, the contributions related to non-zero $a_{0,2}^S$ are possibly nontrivial compared with the ones related to $a_{1,3}^S$, and hence are considered in this work.

3 Numerical Results and Discussions

Before presenting our numerical results, we would like to clarify the input parameters used in the evaluations. For the CKM matrix elements, we adopt the Wolfenstein parameterization and choose the four parameters as [77]

$$A = 0.790_{-0.012}^{+0.017}, \quad \lambda = 0.22650_{-0.00048}^{+0.00048}, \quad \bar{\rho} = 0.141_{-0.017}^{+0.016}, \quad \bar{\eta} = 0.357_{-0.011}^{+0.011}. \quad (47)$$

As for the quark masses, we take [77]

$$m_s(\mu)/m_q(\mu) = 27.3_{-1.3}^{+0.7}, \quad m_s(2\text{GeV}) = 93_{-5}^{+11} \text{ MeV}, \quad m_b(m_b) = 4.18_{-0.02}^{+0.03} \text{ GeV}, \quad (48)$$

$$m_c = 1.67 \pm 0.07 \text{ GeV}, \quad m_b = 4.78 \pm 0.06 \text{ GeV}, \quad m_t = 172.76 \pm 0.30 \text{ GeV}, \quad (49)$$

where $m_q \equiv (m_u + m_d)/2$. For the well-determined Fermi coupling constant, masses of mesons and lifetimes of B mesons, we take their default values given by PDG [77].

The nonperturbative inputs used in this work include decay constant, Gegenbauer moment and form factor. Unfortunately, for the $B_{u,d,s} \rightarrow K_0^*(1430)P$ and $K_0^*(1430)V$ decays concerned in this work, some of these nonperturbative inputs are not known. The standard light-front (SLF) approach [78–81] provides a conceptually simple and phenomenologically feasible framework for calculating the non-perturbative quantities of hadrons. However, it is powerless for determining the zero-mode contributions by itself and the Lorentz covariance is lost. In order to cover the shortages of SLF approach, a manifestly covariant light-front (CLF) approach is exploited [56, 82, 83] with the help of the manifestly covariant Bethe-Salpeter (BS) approach, and has been applied to study the $B_{u,d} \rightarrow SP$ and SV decays [30–33]. Unfortunately, this traditional CLF approach has some self-consistence problems, and the covariance in fact can not be strictly guaranteed due to the residual spurious ω -dependent contribution [56, 84, 85]. In order to resolve these problems, a self-consistent scheme is presented in Ref. [84] by improving the correspondence between CLF and BS calculation, and has been tested in, for instance, Refs. [85–93]. Most of the results based on such improved self-consistent CLF approach for the decay constant and form factors generally agree with the experimental data and the predictions obtained by using Lattice QCD (LQCD) and light cone sum rules (LCSR) (some examples can be found in Refs. [86–90]), while the self-consistent CLF results for some DAs of light P -mesons (for instance, the twist-3 DAs of π and K mesons [93, 94]) are different from the QCD sum rule (QCD SR) results.

In the previous works for $B_{u,d} \rightarrow SP$ and SV decays [30–33], the decay constant and Gegenbauer moments are evaluated by using the QCD SR, while the form factor is evaluated by using the traditional CLF approach. In this work, all of the nonperturbative parameters will be calculated by using the self-consistent CLF approach for consistence. The theoretical framework for the decay constant of S , P and V mesons and the form factors of $P \rightarrow (S, P, V)$ transitions within the CLF approach has been given in, for instance, Refs. [56, 86], and the self-consistent correspondence relation between the BS and the LF approaches has been discussed

in detail in Refs. [84–87, 89, 90, 92, 93]. Using the Gaussian-type wavefunctions ³

$$\psi_{1s}(x, \mathbf{k}_\perp) = \frac{4\pi^{\frac{3}{4}}}{\beta^{\frac{3}{2}}} \sqrt{\frac{\partial k_z}{\partial x}} \exp\left[-\frac{\vec{k}^2}{2\beta^2}\right], \quad (50)$$

$$\psi_{1p}(x, \mathbf{k}_\perp) = \frac{\sqrt{2}}{\beta} \psi_{1s}(x, \mathbf{k}_\perp), \quad (51)$$

$$\psi_{2p}(x, \mathbf{k}_\perp) = \sqrt{\frac{5}{2}} \left(\frac{2\vec{k}^2}{5\beta^2} - 1 \right) \psi_{1p}(x, \mathbf{k}_\perp), \quad (52)$$

and the values of input parameters collected in Ref. [85], we obtain (in units of MeV)

$$f_{K_0^*(1430)} = 18 \pm 5 \quad \text{S1}, \quad f_{K_0^*(1430)} = 43 \pm 10 \quad \text{S2}, \quad (53)$$

$$f_{B_{u,d}} = 186 \pm 7, \quad f_{B_s} = 224 \pm 9, \quad f_\pi = 131 \pm 7, \quad f_K = 156 \pm 5, \quad (54)$$

$$f_{K^*} = 205 \pm 8, \quad f_\rho = 210 \pm 4, \quad f_\omega = 210 \pm 4, \quad f_\phi = 228 \pm 5, \quad (55)$$

$$f_{K^*}^\perp = 173 \pm 6, \quad f_\rho^\perp = 167 \pm 4, \quad f_\omega^\perp = 167 \pm 4, \quad f_\phi^\perp = 198 \pm 4, \quad (56)$$

where, as has been mentioned in the introduction, S1 and S2 are the two assumptions for $K_0^*(1430)$ meson that

- S1: $K_0^*(1430)$ is the first excited p-wave two-quark state;
- S2: $K_0^*(1430)$ is the lowest-lying p-wave two-quark state.

It is found that our result for $f_{K_0^*(1430)}$ in S2 is in agreement with the results $f_{K_0^*} = 34 \pm 7$ MeV [96] and 42 ± 8 MeV [97] obtained within QCD SR and $f_{K_0^*} = 42 \pm 2$ MeV [98] obtained within the finite-energy sum rules. The heavy lepton τ decay process $\tau \rightarrow K_0^*(1430)\nu_\tau$ is very suitable for testing the value of $f_{K_0^*}$ because there is only one hadron evolved in this decay, the interaction in the leptonic vertex can be calculated with high precision, and its branching fraction is dependent on $f_{K_0^*}$ directly. Using our prediction $f_{K_0^*} = 43$ MeV and the formulae given in Ref. [97], we obtain $\mathcal{B}(\tau \rightarrow K_0^*(1430)\nu) \simeq 0.81 \times 10^{-4}$ (S2), which is allowed by current data $\mathcal{B}(\tau \rightarrow K_0^*(1430)\nu)^{\text{exp.}} < 5 \times 10^{-4}$ [77].

Our results for the form factors of $B \rightarrow K_0^*(1430)$, K , K^* , π , ρ , ω and $B_s \rightarrow K_0^*(1430)$, K , K^* , ϕ transitions are collected in Table 1. Our results $U_{0,1}^{B \rightarrow K_0^*} = 0.29 \pm 0.02$ (S2) and 0.18 ± 0.01 (S1) are

³Our sign convention for $\psi_{2p}(x, \mathbf{k}_\perp)$ is different from the one in Ref. [95], and ensures the positive decay constant of $S(2P)$ and form factor of $P \rightarrow S(2P)$ transition. It should be noted that the different conventions do not affect the final results of observables.

Table 1: Form factors of $B \rightarrow K_0^*(1430), K, K^*, \pi, \rho, \omega$ and $B_s \rightarrow K_0^*(1430), K, K^*, \phi$ transitions in S1 (lower entry) and S2 (upper entry) by using the self-consistent CLF approach.

F	$F(0)$	a	b	F	$F(0)$	a	b
$U_1^{B \rightarrow K_0^*}$	0.29 ± 0.02	1.27	0.33	$U_0^{B \rightarrow K_0^*}$	0.29 ± 0.02	0.16	0.11
	0.18 ± 0.01	1.03	0.15		0.18 ± 0.01	-0.23	0.29
$U_1^{B_s \rightarrow K_0^*}$	0.28 ± 0.02	1.58	0.84	$U_0^{B_s \rightarrow K_0^*}$	0.28 ± 0.02	0.55	0.20
	0.23 ± 0.02	0.92	0.29		0.23 ± 0.02	-0.23	0.36
$F_0^{B \rightarrow \pi}$	0.27 ± 0.03	0.65	0.03	$F_0^{B \rightarrow K}$	0.34 ± 0.03	0.66	0.07
$F_0^{B_s \rightarrow K}$	0.23 ± 0.03	0.95	0.28	$A_0^{B \rightarrow \omega}$	0.29 ± 0.03	1.54	0.74
$A_0^{B \rightarrow \rho}$	0.29 ± 0.03	1.54	0.74	$A_0^{B \rightarrow K^*}$	0.34 ± 0.04	1.52	0.65
$A_0^{B_s \rightarrow K^*}$	0.21 ± 0.04	1.94	1.62	$A_0^{B_s \rightarrow \phi}$	0.28 ± 0.04	1.80	1.29

Table 2: Form factors of $B \rightarrow K, K^*, \pi, \rho, \omega$ and $B_s \rightarrow K, K^*, \phi$ transitions at $q^2 = 0 \text{ GeV}^2$ obtained in this and some previous works .

	This work	LCSR	SCET	LFQM	pQCD	CCQM
		[99, 100]	[101]	[102]	[103, 104]	[105]
$F_0^{B \rightarrow \pi}$	0.27 ± 0.03	0.258 ± 0.030	0.247	0.25	$0.26_{-0.05}^{+0.05}$	0.283 ± 0.019
$F_0^{B \rightarrow K}$	0.34 ± 0.03	0.331 ± 0.040	0.297	0.34	$0.31_{-0.05}^{+0.05}$	—
$F_0^{B_s \rightarrow K}$	0.23 ± 0.03	—	0.290	0.23	$0.26_{-0.05}^{+0.05}$	0.247 ± 0.015
$A_0^{B \rightarrow \rho}$	0.29 ± 0.03	0.303 ± 0.028	0.260	0.32	$0.25_{-0.06}^{+0.07}$	0.266 ± 0.013
$A_0^{B \rightarrow \omega}$	0.29 ± 0.03	0.281 ± 0.030	0.240	0.28	$0.23_{-0.05}^{+0.06}$	0.236 ± 0.011
$A_0^{B \rightarrow K^*}$	0.34 ± 0.04	0.374 ± 0.034	0.283	0.38	$0.31_{-0.07}^{+0.09}$	—
$A_0^{B_s \rightarrow K^*}$	0.21 ± 0.04	0.363 ± 0.034	0.279	0.25	$0.24_{-0.05}^{+0.06}$	0.225 ± 0.090
$A_0^{B_s \rightarrow \phi}$	0.28 ± 0.04	0.474 ± 0.037	0.279	0.31	$0.31_{-0.07}^{+0.09}$	—

a little larger and smaller than the traditional CLF results $U_{0,1}^{B \rightarrow K_0^*} = 0.26(\text{S2})$ and $0.21(\text{S1})$ [30]. The results for $B_s \rightarrow K_0^*$ transition are first obtained in this work. The previous results for the $B \rightarrow K, K^*, \pi, \rho, \omega$ and $B_s \rightarrow K, K^*, \phi$ transitions at $q^2 = 0 \text{ GeV}^2$ obtained via

Table 3: Gegenbauer moments of pseudoscalar and vector mesons at $\mu = 1\text{GeV}$.

		a_1	a_2	a_3
π	this work	0	0.10 ± 0.04	0
	LQCD [106]	0	0.116 ± 0.020	0
	QCD SR [107]	0	0.25 ± 0.15	0
	linear(HO) [108]	0	$0.12(0.05)$	0
\bar{K}	this work	0.09 ± 0.01	0.02 ± 0.02	0.05 ± 0.01
	LQCD [106]	$0.053^{+0.031}_{-0.033}$	0.106 ± 0.016	—
	QCD SR [107]	0.06 ± 0.03	0.25 ± 0.15	—
	linear(HO) [108]	$0.09(0.13)$	$0.03(-0.03)$	$0.06(0.04)$
ρ	this work	0	-0.01 ± 0.02	0
	QCD SR [100]	0	$0.09^{+0.10}_{-0.07}$	0
	QCD SR [109]	0	0.15 ± 0.07	0
	linear(HO) [108]	0	$0.02(-0.02)$	0
\bar{K}^*	this work	0.13 ± 0.04	-0.07 ± 0.00	0.02 ± 0.00
	QCD SR [100]	0.10 ± 0.07	$0.07^{+0.09}_{-0.07}$	—
	QCD SR [109]	0.03 ± 0.02	0.11 ± 0.09	—
	linear(HO) [108]	$0.11(0.14)$	$-0.03(-0.07)$	$0.03(0.02)$
ϕ	this work	0	-0.13 ± 0.03	0
	QCD SR [100]	0	$0.06^{+0.09}_{-0.07}$	0
	QCD SR [109]	0	0.18 ± 0.08	0

other approaches are collected in Table 3 for comparison. It can be found that these results based on different approaches are generally consistent with each other except for the large $A_0^{B_s \rightarrow (K^*, \phi)} = (0.363 \pm 0.034, 0.474 \pm 0.037)$ predicted by LCSR [99, 100] (relatively small results $A_0^{B_s \rightarrow (K^*, \phi)} = (0.314 \pm 0.048, 0.389 \pm 0.045)$ are obtained in Ref. [110]). From above discussion and Table 3, we can roughly conclude that the uncertainties of form factors associated with B and B_s decays caused by different approaches are less than about 20% and 35%, respectively.

The DAs of mesons have been studied within the LF approaches in, for instance, Refs. [84, 93, 94]. The Gegenbauer moments can be extracted from DAs via

$$a_n^M = \frac{2(2n+3)}{3(n+1)(n+2)} \int_0^1 dx C_n^{3/2}(x-\bar{x})\Phi(x), \quad (57)$$

Table 4: Gegenbauer moments of $K_0^*(1430)$ at $\mu = 1\text{GeV}$ in S1 (lower entry) and S2 (upper entry).

	a_1	a_2	a_3
this work	-1.65 ± 0.38	-0.38 ± 0.02	-0.06 ± 0.01
	-1.93 ± 0.69	0.75 ± 0.13	-1.13 ± 0.72
QCD SR [30]	-7.21 ± 1.64	—	-5.31 ± 2.70
	7.33 ± 0.89	—	-15.17 ± 1.01

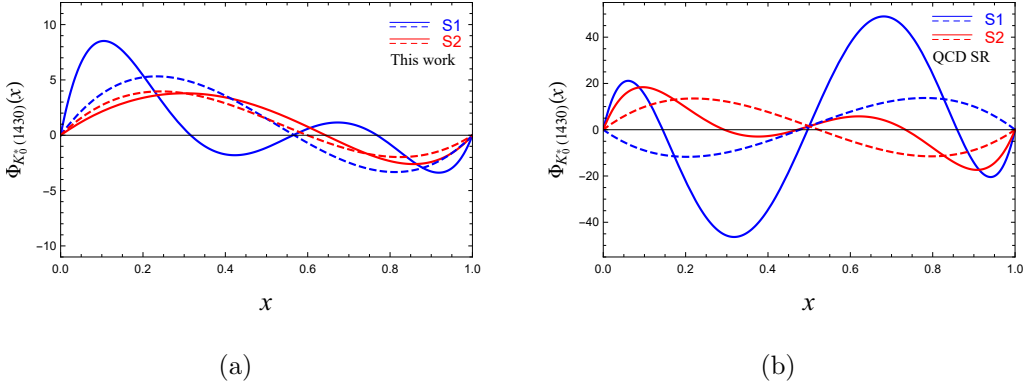


Figure 1: The DA of $K_0^*(1430)$ predicted in this work and QCD SR [30]. The dashed and solid lines correspond to the truncations up to $n = 1$ and $n = 3$, respectively, according to Eq. (81).

where, $C_n^{3/2}$ are Gegenbauer polynomials. Our numerical results for the Gegenbauer moments at $\mu = 1\text{GeV}$ are collected in Tables 3 and 4. The results obtained by using LQCD [106], QCD SR [30,100,107,109] and traditional LFQM with linear confining and harmonic oscillator (HO) potentials [108] are also collected in these tables for comparison. For the pseudoscalar and vector mesons, our results are generally agree with the results based on the other approaches within errors except for the signs of $a_2^{\rho,K^*,\phi}$, which is caused by the fact that the DAs predicted by LF approaches are usually different from the QCD SR predictions especially at $x \rightarrow 0$ or 1 (some examples can be found in, for instance, Refs. [93,108,111]). For the $K_0^*(1430)$ meson, it is found from Table 4 that our results are much smaller than the ones given by QCD SR [30]. In order to clearly show their difference, we plot the DA of $K_0^*(1430)$ in Fig. 2. For the case of $n = 1$ (dashed lines), our results in S1 and S2 are similar, while the QCD SR results in S1 and S2 are totally different with each other due to the different signs of $a_1^{K_0^*}$ (QCD SR, -7.21

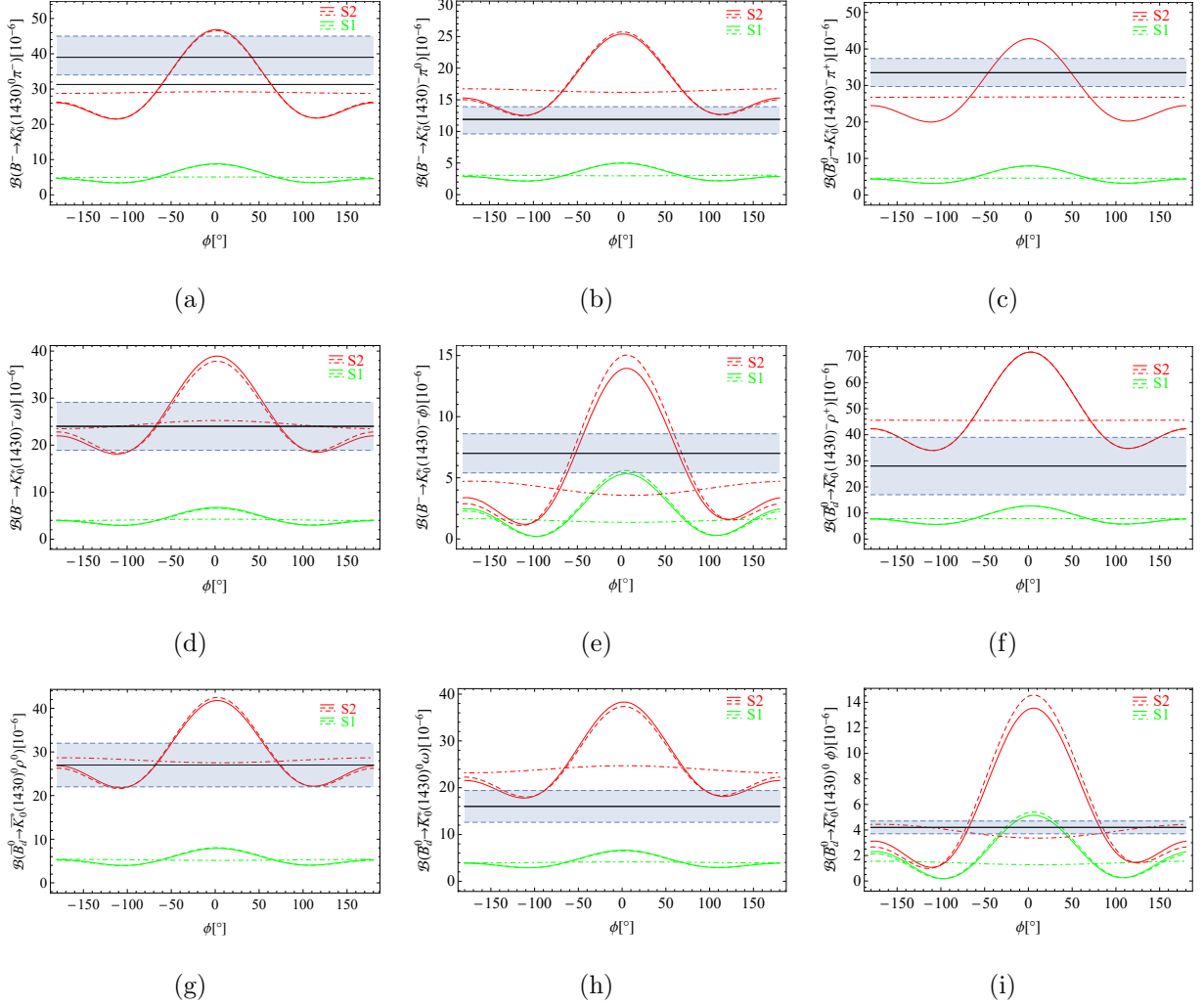


Figure 2: The dependences of measured $\mathcal{B}(B_{u,d,s} \rightarrow K_0^*(1430)(\pi, \rho, \omega, \phi))$ on ϕ_A with $(\rho_A, \rho_H) = (1, 0)$ and ϕ_H with $(\rho_A, \rho_H) = (0, 1)$ are shown by the dash and dash-dotted lines, respectively. The solid lines are plotted with the simplification that $X_H(\rho_H, \phi_H) = X_A(\rho_A, \phi_A)$ with $\rho_A = 1$. The shaded region is the experimental result with 1σ error bar. See text for further discussion.

vs. 7.33). In addition, the $a_3^{K_0^*}$ correction to $\Phi_{K_0^*}(x)$ in our evaluation is not as significant as the one predicted by QCD SR. More theoretical and experimental efforts are needed for a clear picture of $\Phi_{K_0^*}(x)$.⁴

⁴The $\gamma\gamma \rightarrow K_0^{*+}(1430)K_0^{*-}(1430) \rightarrow 2K2\pi$ process may provide a way to test the DA of $K_0^*(1430)$, which is similar to the cases of $\gamma\gamma \rightarrow \pi^+\pi^-$ and K^+K^- processes for testing the DAs of π and K mesons [112, 113]. Such process is in the scope of Belle(-II) in principle [114], but the specific measurement has not been made.

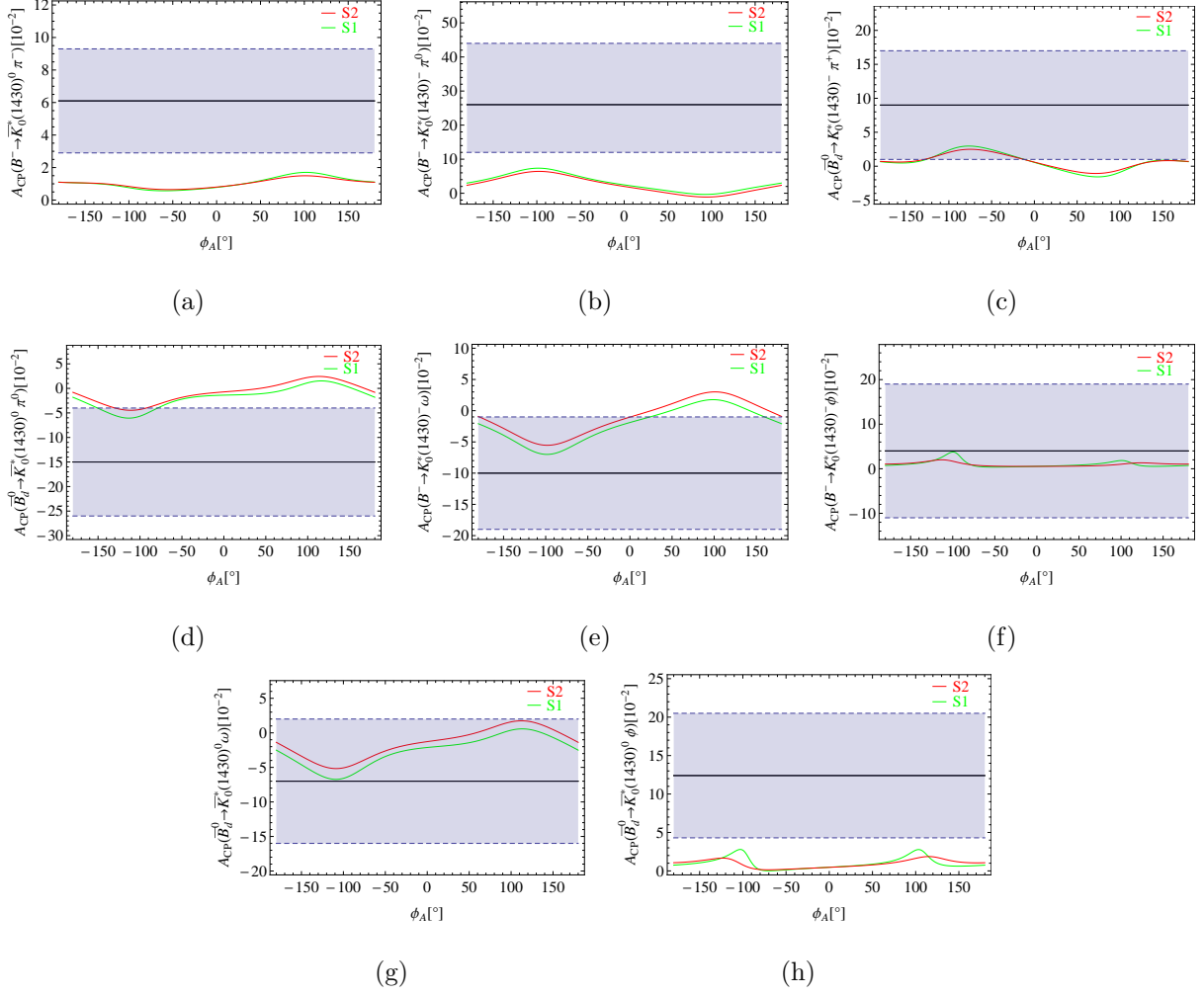


Figure 3: The dependences of measured $A_{CP}(B_{u,d} \rightarrow K_0^*(1430)(\pi, \rho, \omega, \phi))$ on ϕ_A with $\rho_A = 1$ in S1 and S2. The shaded region is the experimental result with 1σ error bar. See text for further discussion.

Using the inputs given above, we then present our numerical results and discussion. The QCDF approach itself cannot give the exact values of the end-point parameters $X_H(\rho_H, \phi_H)$ in the hard-spectator scattering corrections and $X_A(\rho_A, \phi_A)$ in the annihilation amplitudes, which can only be determined by fitting to the experimental data. The current data indicate that $\rho_{A(H)}$ is at the level of 1, but $\phi_{A(H)}$ is generally different for kinds of decay types. For instance, $\phi_A = -55^\circ, -22^\circ$ and -70° with $\rho_A = 1$ (the so-called ‘‘Scenario S4’’ in Ref. [70]) are favored by the $B \rightarrow PP, PV$ and VP decays, respectively [70–72]. In order to clearly show the effects of end-point contributions, we plot the dependences of the measured $\mathcal{B}(B_{u,d} \rightarrow K_0^*(1430)(\pi, \rho, \omega, \phi))$

on the end-point parameters in Fig. 2, in addition, the experimental data are also shown in such figure for comparison. The dash and dash-dotted lines show the dependences on ϕ_A with $(\rho_A, \rho_H) = (1, 0)$ and ϕ_H with $(\rho_A, \rho_H) = (0, 1)$, respectively. Comparing the dash with the dash-dotted lines, it can be found that the measured decay modes are very sensitive to $X_A(\rho_A, \phi_A)$, but the effect of $X_H(\rho_H, \phi_H)$ is trivial. It can be easily understood because these decay modes are penguin-dominated, and the hard-spectator scattering corrections may be significant only when the decays are dominated by the color-suppressed tree contribution [70]. Therefore, we assume that the end-point parameters are universal in the annihilation and hard-spectator scattering corrections, *i.e.*, $X_H(\rho_H, \phi_H) = X_A(\rho_A, \phi_A)$, in our following discussions for simplification.⁵ Under this assumption, the dependences of the measured branching fractions and direct CP asymmetries of $B_{u,d} \rightarrow K_0^*(1430)(\pi, \rho, \omega, \phi)$ decays on the end-point parameters are shown in Figs. 2 and 3 (solid lines), respectively.

- From Figs. 2 and 3, it can be found that the scenarios S1 and S2 give significantly different results for the branching fractions, but the direct CP asymmetries are similar with each other. As shown by Fig. 2, the results based on S2 could agree well with the experimental data at the level of 1σ when a proper value of ϕ_A is taken; however, the results for most of decay modes based on S1 are much smaller than data for any value of ϕ_A . This implies that the measured $B_{u,d} \rightarrow K_0^*(1430)P$ and $K_0^*(1430)V$ decays favor $K_0^*(1430)$ as the lowest-lying ($s, u/d$) state rather than it as the first excited one. In addition, this conclusion would not change even if the 20% uncertainties of form factors caused by different approaches are considered. Therefore, our following discussion is mainly based on S2, unless otherwise stated.
- In S2, it can be found from Figs. 2 that $\phi_A \sim [-50^\circ, -100^\circ]$ and $[50^\circ, 100^\circ]$ is allowed by the branching fractions, while a negative ϕ_A is favored by the CP asymmetries as shown by Fig. 3. In our following numerical calculation, we take

$$(\rho_A, \phi_A) = (1, -55^\circ) \quad \text{and} \quad (1, -64^\circ) \quad (58)$$

for $B \rightarrow SP$ and SV decay modes, respectively.

⁵In the decay modes considered in this work, $\bar{B}_s \rightarrow K_0^{*0}(\pi^0, \rho^0, \omega)$ decays are color-suppressed tree dominated, thus the simplification $X_H(\rho_H, \phi_H) = X_A(\rho_A, \phi_A)$ may affect our following predictions for these decays.

Table 5: Branching fractions (in units of 10^{-6}) of $B_{u,d,s} \rightarrow K_0^*(1430)P$ ($P = \pi, K$) decays.

Decay modes	S2	S1	QCDF(S2)	pQCD	data
$B^- \rightarrow K_0^*(1430)^- K^0$	$0.08_{-0.00-0.02-0.03}^{+0.00+0.01+0.03}$	$0.06_{-0.00-0.01-0.03}^{+0.00+0.01+0.04}$	$0.11_{-0.04}^{+0.05}$ [29]	0.38 ± 0.22 [116]	
$B^- \rightarrow K_0^*(1430)^0 K^-$	$3.19_{-0.14-0.62-1.39}^{+0.18+0.36+1.73}$	$0.54_{-0.02-0.11-0.27}^{+0.03+0.06+0.35}$	$3.37_{-0.85}^{+1.03}$ [29]	3.99 ± 1.38 [116]	0.38 ± 0.13
$B^- \rightarrow \bar{K}_0^*(1430)^0 \pi^-$	$33.37_{-1.04-7.29-14.95}^{+1.48+4.28+18.52}$	$5.85_{-0.18-1.27-2.99}^{+0.26+0.75+3.88}$	$12.9_{-3.7}^{+4.6}$ [33]	$47.6_{-10.1}^{+11.3}$ [117] 36.6 ± 11.3 [116]	39_{-5}^{+6}
$B^- \rightarrow K_0^*(1430)^- \pi^0$	$18.42_{-0.58-3.73-7.80}^{+0.82+2.18+9.52}$	$3.41_{-0.11-0.67-1.61}^{+0.15+0.39+2.03}$	$7.4_{-1.9}^{+2.4}$ [33]	$28.8_{-6.1}^{+6.8}$ [117] 12.7 ± 4.2 [116]	$11.9_{-2.3}^{+2.0}$
$\bar{B}_d^0 \rightarrow \bar{K}_0^*(1430)^0 K^0$	$0.08_{-0.00-0.02-0.03}^{+0.00+0.01+0.04}$	$0.06_{-0.00-0.01-0.03}^{+0.00+0.01+0.04}$	$0.24_{-0.09}^{+0.12}$ [29]	0.49 ± 0.33 [116]	
$\bar{B}_d^0 \rightarrow K_0^*(1430)^0 \bar{K}^0$	$2.97_{-0.13-0.57-1.29}^{+0.16+0.33+1.61}$	$0.50_{-0.02-0.10-0.25}^{+0.03+0.06+0.33}$	$4.05_{-1.08}^{+1.34}$ [29]	4.61 ± 1.50 [116]	
$\bar{B}_d^0 \rightarrow K_0^*(1430)^- K^+$	$0.08_{-0.01-0.02-0.03}^{+0.01+0.02+0.04}$	$0.02_{-0.00-0.00-0.01}^{+0.00+0.00+0.01}$	$0.11_{-0.05}^{+0.07}$ [29]	0.09 ± 0.06 [116]	
$\bar{B}_d^0 \rightarrow K_0^*(1430)^+ K^-$	$0.09_{-0.01-0.03-0.04}^{+0.01+0.02+0.05}$	$0.05_{-0.00-0.01-0.03}^{+0.00+0.01+0.04}$	$0.06_{-0.03}^{+0.05}$ [29]	0.62 ± 0.40 [116]	
$\bar{B}_d^0 \rightarrow K_0^*(1430)^- \pi^+$	$30.55_{-0.97-6.56-13.70}^{+1.36+3.85+16.97}$	$5.31_{-0.17-1.13-2.72}^{+0.24+0.66+3.52}$	$13.8_{-3.6}^{+4.5}$ [33]	$43.0_{-9.1}^{+10.2}$ [117] 33.4 ± 10.2 [116]	$33.5_{-3.8}^{+3.9}$
$\bar{B}_d^0 \rightarrow \bar{K}_0^*(1430)^0 \pi^0$	$13.78_{-0.44-3.20-6.54}^{+0.61+1.89+8.24}$	$2.26_{-0.07-0.54-1.25}^{+0.10+0.32+1.68}$	$5.6_{-1.3}^{+2.6}$ [33]	$18.4_{-3.9}^{+4.4}$ [117] 22.4 ± 6.6 [116]	
$\bar{B}_s^0 \rightarrow \bar{K}_0^*(1430)^0 K^0$	$29.70_{-0.93-6.37-13.32}^{+1.31+3.74+16.51}$	$5.40_{-0.17-1.13-2.76}^{+0.24+0.66+3.59}$			
$\bar{B}_s^0 \rightarrow K_0^*(1430)^0 \bar{K}^0$	$3.08_{-0.10-0.72-1.17}^{+0.14+0.44+1.51}$	$1.22_{-0.04-0.35-0.59}^{+0.05+0.22+0.78}$			
$\bar{B}_s^0 \rightarrow K_0^*(1430)^- K^+$	$29.79_{-0.95-6.30-13.36}^{+1.33+3.70+16.56}$	$5.37_{-0.17-1.11-2.75}^{+0.24+0.65+3.57}$			
$\bar{B}_s^0 \rightarrow K_0^*(1430)^+ K^-$	$3.94_{-0.13-0.79-1.21}^{+0.18+0.47+1.57}$	$1.82_{-0.07-0.40-0.63}^{+0.09+0.24+0.81}$			
$\bar{B}_s^0 \rightarrow K_0^*(1430)^+ \pi^-$	$6.41_{-0.44-0.02-1.14}^{+0.49+0.04+1.22}$	$4.51_{-0.31-0.01-0.91}^{+0.35+0.01+0.98}$		$37.0_{-10.0}^{+14.0}$ [51]	
$\bar{B}_s^0 \rightarrow K_0^*(1430)^0 \pi^0$	$0.70_{-0.04-0.12-0.26}^{+0.05+0.07+0.31}$	$0.21_{-0.01-0.03-0.07}^{+0.01+0.02+0.09}$		$0.41_{-0.07}^{+0.10}$ [51]	

Using the values of end-point parameters given above, we then present our numerical results and discussions. The branching fractions and the direct CP asymmetries of $B_{u,d,s} \rightarrow K_0^*(1430)P$ ($P = \pi, K$) and $K_0^*(1430)V$ ($V = K^*, \rho, \omega, \phi$) decays are given in tables 5, 6, 7, 8, 9 and 10. For each result, the first error is caused by the uncertainties of CKM parameters, the second error comes from the variation of quark masses, and the third error from the decay constants, form factors and Gegenbauer moments. In each table, the experimental data given by PDG [77] or HFAG [115] and the theoretical results obtained in previous works are also listed for comparison.

- From tables 5 and 6, it can be found that the branching fractions obtained based on S2 are

Table 6: Branching fractions (in units of 10^{-6}) of $B_{u,d,s} \rightarrow K_0^*(1430)V$ ($V = K^*, \rho, \omega, \phi$) decays.

Decay modes	S2	S1	QCDF(S2)	pQCD(S2)	data
$B^- \rightarrow K_0^*(1430)^- K^{*0}$	$0.24_{-0.01}^{+0.01+0.01+0.05}$	$0.07_{-0.00}^{+0.00+0.00+0.01}$	$0.01_{-0.01}^{+0.01}$ [29]	$1.3_{-0.3}^{+0.5}$ [45]	
$B^- \rightarrow K_0^*(1430)^0 K^{*-}$	$2.48_{-0.11}^{+0.14+0.30+1.38}$	$0.43_{-0.02}^{+0.02+0.05+0.29}$	$2.17_{-0.47}^{+0.55}$ [29]	$1.5_{-0.3}^{+0.5}$ [45]	
$B^- \rightarrow \bar{K}_0^*(1430)^0 \rho^-$	$51.81_{-1.62}^{+2.29+5.64+28.39}$	$8.66_{-0.27}^{+0.38+0.97+5.71}$	$39.0_{-35.8}^{+34.5}$ [33]	$12.1_{-0.0}^{+2.8}$ [52]	
$B^- \rightarrow K_0^*(1430)^- \rho^0$	$20.99_{-0.66}^{+0.93+2.55+12.72}$	$3.15_{-0.10}^{+0.14+0.41+2.44}$	$14.8_{-3.2}^{+3.7}$ [33]	$8.4_{-0.0}^{+2.3}$ [52]	
$B^- \rightarrow K_0^*(1430)^- \omega$	$25.08_{-0.78}^{+1.11+2.82+13.98}$	$4.11_{-0.13}^{+0.18+0.48+2.79}$	$21.5_{-4.9}^{+5.8}$ [33]	$7.4_{-1.5}^{+2.1}$ [52]	24.0 ± 5.1
$B^- \rightarrow K_0^*(1430)^- \phi$	$4.97_{-0.16}^{+0.22+0.21+1.08}$	$1.29_{-0.04}^{+0.06+0.08+0.35}$	$3.80_{-0.6}^{+0.7}$ [33]	$25.6_{-5.4}^{+6.2}$ [118]	7.0 ± 1.6
$\bar{B}_d^0 \rightarrow \bar{K}_0^*(1430)^0 K^{*0}$	$0.22_{-0.01}^{+0.01+0.01+0.05}$	$0.06_{-0.00}^{+0.00+0.00+0.01}$			< 3.3
$\bar{B}_d^0 \rightarrow K_0^*(1430)^0 \bar{K}^{*0}$	$2.30_{-0.10}^{+0.13+0.28+1.28}$	$0.39_{-0.02}^{+0.02+0.05+0.26}$	$2.01_{-0.45}^{+0.54}$ [29]		
$\bar{B}_d^0 \rightarrow K_0^*(1430)^- K^{*+}$	$0.03_{-0.00}^{+0.00+0.00+0.02}$	$0.01_{-0.00}^{+0.00+0.00+0.01}$	$0.18_{-0.08}^{+0.13}$ [29]		
$\bar{B}_d^0 \rightarrow K_0^*(1430)^+ K^{*-}$	$0.04_{-0.00}^{+0.00+0.00+0.03}$	$0.05_{-0.00}^{+0.00+0.00+0.04}$	$0.01_{-0.01}^{+0.01}$ [29]		
$\bar{B}_d^0 \rightarrow K_0^*(1430)^- \rho^+$	$45.92_{-1.43}^{+2.03+5.05+25.14}$	$7.67_{-0.24}^{+0.34+0.86+5.05}$	$36.3_{-7.4}^{+8.5}$ [33]	$10.5_{-0.0}^{+2.7}$ [52]	28.0 ± 11.0
$\bar{B}_d^0 \rightarrow \bar{K}_0^*(1430)^0 \rho^0$	$27.95_{-0.87}^{+1.24+2.78+13.95}$	$5.10_{-0.16}^{+0.23+0.50+2.91}$	$23.4_{-4.5}^{+5.1}$ [33]	$4.8_{-0.0}^{+1.1}$ [52]	27.0 ± 5.0
$\bar{B}_d^0 \rightarrow \bar{K}_0^*(1430)^0 \omega$	$24.71_{-0.78}^{+1.10+2.74+13.76}$	$4.06_{-0.13}^{+0.18+0.46+2.75}$	$21.9_{-5.0}^{+5.9}$ [33]	$9.3_{-2.0}^{+2.1}$ [52]	16.0 ± 3.4
$\bar{B}_d^0 \rightarrow \bar{K}_0^*(1430)^0 \phi$	$4.80_{-0.15}^{+0.21+0.21+1.46}$	$1.25_{-0.04}^{+0.06+0.08+0.42}$	$3.7_{-0.6}^{+0.8}$ [33]	$23.6_{-5.0}^{+5.6}$ [118]	4.2 ± 0.5
$\bar{B}_s^0 \rightarrow \bar{K}_0^*(1430)^0 K^{*0}$	$29.87_{-0.93}^{+1.32+3.28+17.95}$	$5.08_{-0.16}^{+0.22+0.56+3.57}$			
$\bar{B}_s^0 \rightarrow K_0^*(1430)^0 \bar{K}^{*0}$	$5.11_{-0.16}^{+0.23+0.29+1.43}$	$2.15_{-0.07}^{+0.09+0.07+0.50}$			
$\bar{B}_s^0 \rightarrow K_0^*(1430)^- K^{*+}$	$28.39_{-0.89}^{+1.26+3.15+17.04}$	$4.83_{-0.15}^{+0.21+0.54+3.39}$			
$\bar{B}_s^0 \rightarrow K_0^*(1430)^+ K^{*-}$	$5.42_{-0.21}^{+0.28+0.32+1.63}$	$2.17_{-0.11}^{+0.13+0.08+0.51}$			
$\bar{B}_s^0 \rightarrow K_0^*(1430)^+ \rho^-$	$17.77_{-1.22}^{+1.36+0.12+2.74}$	$12.57_{-0.86}^{+0.97+0.05+2.30}$		108_{-23}^{+25} [53]	
$\bar{B}_s^0 \rightarrow K_0^*(1430)^0 \rho^0$	$1.28_{-0.09}^{+0.10+0.11+0.56}$	$0.35_{-0.02}^{+0.03+0.02+0.16}$		$0.96_{-0.20}^{+0.22}$ [53]	
$\bar{B}_s^0 \rightarrow K_0^*(1430)^0 \omega$	$1.45_{-0.10}^{+0.11+0.12+0.57}$	$0.44_{-0.03}^{+0.03+0.03+0.17}$		$0.86_{-0.18}^{+0.21}$ [53]	
$\bar{B}_s^0 \rightarrow K_0^*(1430)^0 \phi$	$1.90_{-0.08}^{+0.11+0.22+1.03}$	$0.35_{-0.01}^{+0.02+0.04+0.21}$		$0.95_{-0.17}^{+0.25}$ [53]	

generally much larger than the ones based on S1 because relatively larger decay constant of $K_0^*(1430)$ and form factors of $B \rightarrow K_0^*(1430)$ transition are predicated in S2. In addition, most of predictions based on S2 (S1) are favored (disfavored) by experimental data, the only exception is $B^- \rightarrow K_0^*(1430)^0 K^-$ decay. Our result $\mathcal{B}(B^- \rightarrow K_0^*(1430)^0 K^-) = (3.19_{-0.14}^{+0.18+0.36+1.73}) \times 10^{-6}$ in S2 is consistent with the results obtained in the previous works, $(3.37_{-0.85}^{+1.03}) \times 10^{-6}$ (QCDF) [29] and $(3.99 \pm 1.38) \times 10^{-6}$ (pQCD) [116], however all of these theoretical predictions are an order of magnitude larger than experimental data

Table 7: The direct CP asymmetries (in units of %) of $B_{u,d,s} \rightarrow K_0^*(1430)P$ ($P = \pi, K$) decays.

Decay modes	S2	S1	QCDF(S2)	pQCD(S2)	data
$B^- \rightarrow K_0^*(1430)^- K^0$	$30.32_{-1.11-0.42-1.43}^{+1.08+0.73+1.23}$	$18.58_{-0.72-0.79-1.94}^{+0.71+1.79+2.67}$	$-22.51_{-7.57}^{+4.90}$ [29]		
$B^- \rightarrow K_0^*(1430)^0 K^-$	$-16.56_{-0.63-0.56-0.84}^{+0.64+0.28+0.88}$	$-12.25_{-0.47-1.47-2.25}^{+0.48+1.42+2.23}$	$-2.60_{-1.76}^{+1.61}$ [29]		10 ± 17
$B^- \rightarrow \bar{K}_0^*(1430)^0 \pi^-$	$0.65_{-0.02-0.01-0.06}^{+0.02+0.02+0.05}$	$0.57_{-0.02-0.07-0.13}^{+0.02+0.07+0.13}$	$1.3_{-0.1}^{+0.1}$ [33]		6.1 ± 3.2
$B^- \rightarrow K_0^*(1430)^- \pi^0$	$4.71_{-0.15-0.14-0.34}^{+0.15+0.30+0.43}$	$5.20_{-0.16-0.18-0.46}^{+0.16+0.37+0.64}$	$3.0_{-0.4}^{+0.4}$ [33]	3.5 [117]	26_{-14}^{+18}
$\bar{B}_d^0 \rightarrow \bar{K}_0^*(1430)^0 K^0$	$0.68_{-0.03-1.48-2.62}^{+0.03+3.08+1.34}$	$0.08_{-0.00-0.97-1.81}^{+0.00+2.05+0.81}$			
$\bar{B}_d^0 \rightarrow K_0^*(1430)^0 \bar{K}^0$	$-20.75_{-0.77-0.28-0.59}^{+0.79+0.13+0.61}$	$-19.68_{-0.72-1.35-1.29}^{+0.74+1.27+1.38}$			
$\bar{B}_d^0 \rightarrow K_0^*(1430)^- K^+$	$-1.38_{-0.05-0.38-0.28}^{+0.05+0.16+0.28}$	$-9.01_{-0.32-1.77-4.43}^{+0.32+0.80+4.82}$			
$\bar{B}_d^0 \rightarrow K_0^*(1430)^+ K^-$	$1.46_{-0.06-0.15-0.16}^{+0.06+0.33+0.14}$	$3.56_{-0.14-0.13-1.46}^{+0.14+0.25+0.79}$			
$\bar{B}_d^0 \rightarrow K_0^*(1430)^- \pi^+$	$2.25_{-0.07-0.09-0.16}^{+0.07+0.21+0.17}$	$2.59_{-0.08-0.22-0.53}^{+0.08+0.31+0.50}$	$0.21_{-0.06}^{+0.06}$ [33]		9 ± 8
$\bar{B}_d^0 \rightarrow \bar{K}_0^*(1430)^0 \pi^0$	$-2.04_{-0.06-0.16-0.54}^{+0.06+0.07+0.38}$	$-2.42_{-0.08-0.31-1.11}^{+0.08+0.23+0.85}$	$-1.9_{-0.5}^{+0.4}$ [33]		-15 ± 11
$\bar{B}_s^0 \rightarrow \bar{K}_0^*(1430)^0 K^0$	$0.82_{-0.03-0.00-0.05}^{+0.03+0.01+0.04}$	$0.77_{-0.02-0.06-0.10}^{+0.02+0.06+0.09}$			
$\bar{B}_s^0 \rightarrow K_0^*(1430)^0 \bar{K}^0$	$0.03_{-0.00-0.07-0.04}^{+0.00+0.04+0.06}$	$0.17_{-0.01-0.14-0.10}^{+0.01+0.06+0.15}$			
$\bar{B}_s^0 \rightarrow K_0^*(1430)^- K^+$	$1.25_{-0.04-0.19-0.14}^{+0.04+0.41+0.14}$	$1.78_{-0.06-0.28-0.86}^{+0.06+0.50+0.77}$			
$\bar{B}_s^0 \rightarrow K_0^*(1430)^+ K^-$	$-63.79_{-1.56-6.56-4.83}^{+1.59+3.12+7.34}$	$-61.91_{-1.83-8.20-2.54}^{+1.80+3.82+8.67}$			
$\bar{B}_s^0 \rightarrow K_0^*(1430)^+ \pi^-$	$25.23_{-0.91-2.83-6.57}^{+0.92+1.51+6.69}$	$15.14_{-0.55-1.72-6.37}^{+0.55+0.92+6.42}$		$21.0_{-3.1}^{+3.4}$ [51]	
$\bar{B}_s^0 \rightarrow K_0^*(1430)^0 \pi^0$	$-58.32_{-1.80-1.62-4.91}^{+1.82+3.32+3.83}$	$-71.72_{-2.16-1.97-10.12}^{+2.14+4.17+10.77}$		$95.5_{-8.7}^{+1.2}$ [51]	

$(0.38 \pm 0.13) \times 10^{-6}$. The reason will be analyzed in the next item.

- $B^- \rightarrow K_0^*(1430)^0 K^-$ and $K_0^*(1430)^- K^0$ decays are penguin dominated. After neglecting the power suppressed contribution, their simplified amplitudes can be written as

$$\mathcal{A}(B^- \rightarrow K_0^*(1430)^0 K^-) \sim (a_4^p - \gamma_\chi^{K_0^*0} a_6^p) A_{K-K_0^*(1430)^0}, \quad (59)$$

$$\mathcal{A}(B^- \rightarrow K_0^*(1430)^- K^0) \sim (a_4^p - \gamma_\chi^{K^0} a_6^p) A_{K_0^*(1430)^0 K^-}. \quad (60)$$

A significant feature of scalar meson is that its chiral factor is proportional to $M_S^2/(m_1(\mu) - m_2(\mu))$, which results in that $\gamma_\chi^{K_0^*0}$ is much larger than $\gamma_\chi^{K^0}$. Numerically, we obtain $\gamma_\chi^{K_0^*0} : \gamma_\chi^{K^0} \approx 12.6 : 1.4$ at $\mu \sim m_b$. As a result, it is expected that $\mathcal{B}(B^- \rightarrow K_0^*(1430)^0 K^-) \gg \mathcal{B}(B^- \rightarrow K_0^*(1430)^- K^0)$. Moreover, for all of the penguin dominated $B \rightarrow SP$ and SV decays, the decay modes with $M_2 = S$ (M_2 is the emitted meson) generally have relatively larger branching fractions than the ones with $M_2 = (P, V)$, which can also be found from the numerical results listed in tables 5 and 6.

Table 8: The direct CP asymmetries (in units of %) of $B_{u,d,s} \rightarrow K_0^*(1430)V$ ($V = K^*, \rho, \omega, \phi$) decays.

Decay modes	S2	S1	QCDF(S2)	pQCD(S2)	data
$B^- \rightarrow K_0^*(1430)^- K^{*0}$	$-13.24^{+0.46+0.39+2.34}_{-0.45-0.77-2.36}$	$-11.37^{+0.39+1.24+6.04}_{-0.38-1.46-5.30}$	$-31.02^{+4.67}_{-6.56}$ [29]	$-34.9^{+5.0}_{-4.5}$ [45]	
$B^- \rightarrow K_0^*(1430)^0 K^{*-}$	$-19.99^{+0.75+0.19+0.66}_{-0.73-0.10-0.66}$	$-26.27^{+0.94+1.19+3.06}_{-0.92-1.28-3.02}$	$0.64^{+2.54}_{-2.64}$ [29]	$-67.9^{+4.9}_{-5.2}$ [45]	
$B^- \rightarrow \bar{K}_0^*(1430)^0 \rho^-$	$1.02^{+0.03+0.01+0.03}_{-0.03-0.00-0.03}$	$1.13^{+0.04+0.06+0.17}_{-0.04-0.06-0.16}$	$0.32^{+0.34}_{-0.29}$ [33]	$-7.1^{+0.0}_{-0.0}$ [52]	
$B^- \rightarrow K_0^*(1430)^- \rho^0$	$-4.64^{+0.14+0.18+0.65}_{-0.14-0.39-0.93}$	$-6.10^{+0.19+0.30+1.09}_{-0.19-0.64-1.88}$	$1.6^{+0.6}_{-0.6}$ [33]	$6.3^{+0.0}_{-0.1}$ [52]	
$B^- \rightarrow K_0^*(1430)^- \omega$	$-4.25^{+0.13+0.14+0.53}_{-0.13-0.32-0.73}$	$-5.34^{+0.17+0.23+0.83}_{-0.17-0.47-1.32}$	$0.55^{+0.35}_{-0.34}$ [33]	$6.2^{+0.0}_{-0.0}$ [52]	-10 ± 9
$B^- \rightarrow K_0^*(1430)^- \phi$	$0.68^{+0.02+0.05+0.17}_{-0.02-0.02-0.16}$	$0.42^{+0.01+0.07+0.46}_{-0.01-0.06-0.47}$	$0.64^{+0.02}_{-0.03}$ [33]	1.9 [118]	4 ± 15
$\bar{B}_d^0 \rightarrow \bar{K}_0^*(1430)^0 K^{*0}$	$-3.95^{+0.14+0.50+2.61}_{-0.14-1.01-3.21}$	$-4.49^{+0.16+1.78+5.25}_{-0.16-2.04-5.59}$			
$\bar{B}_d^0 \rightarrow K_0^*(1430)^0 \bar{K}^{*0}$	$-15.78^{+0.60+0.38+0.64}_{-0.59-0.17-0.61}$	$-15.61^{+0.59+1.40+1.07}_{-0.58-1.36-1.05}$			
$\bar{B}_d^0 \rightarrow K_0^*(1430)^- K^{*+}$	$-5.10^{+0.19+0.19+0.35}_{-0.20-0.38-0.39}$	$-1.37^{+0.06+0.64+1.74}_{-0.06-0.30-2.18}$		-83.9 ± 0.7 [45]	
$\bar{B}_d^0 \rightarrow K_0^*(1430)^+ K^{*-}$	$-4.27^{+0.16+0.14+0.43}_{-0.16-0.29-0.52}$	$-3.64^{+0.14+0.02+0.61}_{-0.18-0.03-0.68}$		$38.5^{+1.1}_{-0.8}$ [45]	
$\bar{B}_d^0 \rightarrow K_0^*(1430)^- \rho^+$	$-0.15^{+0.00+0.05+0.15}_{-0.00-0.11-0.16}$	$-0.30^{+0.01+0.08+0.27}_{-0.01-0.15-0.30}$	$1.1^{+0.0}_{-0.0}$ [33]	$-4.8^{+0.3}_{-0.0}$ [52]	
$\bar{B}_d^0 \rightarrow \bar{K}_0^*(1430)^0 \rho^0$	$4.85^{+0.15+0.13+0.53}_{-0.15-0.06-0.39}$	$5.64^{+0.18+0.21+0.87}_{-0.18-0.10-0.59}$	$0.54^{+0.45}_{-0.46}$ [33]	$-24.2^{+0.2}_{-0.0}$ [52]	
$\bar{B}_d^0 \rightarrow \bar{K}_0^*(1430)^0 \omega$	$-3.30^{+0.10+0.09+0.44}_{-0.10-0.19-0.63}$	$-4.24^{+0.13+0.23+0.73}_{-0.13-0.35-1.18}$	$0.03^{+0.37}_{-0.35}$ [33]	$10.0^{+0.1}_{-0.0}$ [52]	-7 ± 9
$\bar{B}_d^0 \rightarrow \bar{K}_0^*(1430)^0 \phi$	$0.15^{+0.00+0.06+0.20}_{-0.00-0.03-0.14}$	$0.03^{+0.00+0.10+0.40}_{-0.00-0.09-0.30}$	$0.43^{+0.04}_{-0.04}$ [33]		12.4 ± 8.1
$\bar{B}_s^0 \rightarrow \bar{K}_0^*(1430)^0 K^{*0}$	$0.68^{+0.02+0.00+0.04}_{-0.02-0.01-0.06}$	$0.67^{+0.02+0.05+0.06}_{-0.02-0.05-0.07}$			
$\bar{B}_s^0 \rightarrow K_0^*(1430)^0 \bar{K}^{*0}$	$0.20^{+0.01+0.05+0.17}_{-0.01-0.02-0.13}$	$0.54^{+0.02+0.10+0.20}_{-0.02-0.09-0.20}$			
$\bar{B}_s^0 \rightarrow K_0^*(1430)^- K^{*+}$	$0.41^{+0.01+0.09+0.17}_{-0.01-0.19-0.21}$	$0.15^{+0.00+0.13+0.45}_{-0.00-0.28-0.54}$		$1.7^{+0.3}_{-0.4}$ [45]	
$\bar{B}_s^0 \rightarrow K_0^*(1430)^+ K^{*-}$	$-46.13^{+1.54+0.32+2.53}_{-1.49-0.31-1.11}$	$-36.91^{+1.47+3.09+12.56}_{-1.44-2.53-10.14}$		$-63.6^{+10.7}_{-8.4}$ [45]	
$\bar{B}_s^0 \rightarrow K_0^*(1430)^+ \rho^-$	$15.11^{+0.63+0.87+4.48}_{-0.61-1.61-4.37}$	$6.85^{+0.29+0.67+2.92}_{-0.28-0.94-2.86}$		$12.6^{+0.0}_{-0.0}$ [53]	
$\bar{B}_s^0 \rightarrow K_0^*(1430)^0 \rho^0$	$-7.83^{+0.25+2.14+8.79}_{-0.25-1.02-6.17}$	$8.98^{+0.29+3.37+15.96}_{-0.28-3.47-11.94}$		$84.5^{+0.1}_{-0.1}$ [53]	
$\bar{B}_s^0 \rightarrow K_0^*(1430)^0 \omega$	$-5.01^{+0.22+1.50+8.30}_{-0.24-3.11-11.42}$	$-26.89^{+1.14+2.24+13.59}_{-1.24-3.71-17.23}$		$-86.7^{+0.1}_{-0.1}$ [53]	
$\bar{B}_s^0 \rightarrow K_0^*(1430)^0 \phi$	$-13.11^{+0.50+0.44+0.93}_{-0.49-0.20-0.80}$	$-11.48^{+0.43+1.27+1.49}_{-0.42-1.14-1.30}$			

In addition, the large $\gamma_{\chi}^{K^*0}$ also results in the large theoretical predictions for $\mathcal{B}(B^- \rightarrow K_0^*(1430)^0 K^-)$ compared with data, which has been mentioned in the last item. It should be noted that the significance of data, $(0.38 \pm 0.13) \times 10^{-6}$, is smaller than 3σ , thus more precise measurement on $\mathcal{B}(B^- \rightarrow K_0^*(1430)^0 K^-)$ is required for confirming or refuting such possible anomaly.

- The $\bar{B}_d^0 \rightarrow K_0^*(1430)^- K^{(*)+}$ and $K_0^*(1430)^+ K^{(*)-}$ decays are pure annihilation processes, and thus are very suitable for probing the effects of annihilation corrections. However,

these decays have very small branching fractions $\sim 10^{-7}$ because their amplitudes are power suppressed, and therefore are not easy to be precisely measured in the near future.

- The $\bar{B}_s^0 \rightarrow K_0^*(1430)^+ \pi^- / \rho^-$ and $\bar{B}_s^0 \rightarrow K_0^*(1430)^0 \pi^0 / \rho^0(\omega)$ decays are tree-dominated, while the former are color-allowed and the later are color-suppressed. As a result, the branching fractions of former are an order of magnitude larger than the later.
- The $SU(3)$ flavor symmetry indicates some useful relations between the decays considered in this work. Taking $B_{u,d,s} \rightarrow SP$ decays as examples, after applying $SU(3)$ flavor symmetry on the spectator quark, one may expect that

$$\mathcal{A}(B^- \rightarrow K_0^*(1430)^- K^0) \approx \mathcal{A}(\bar{B}_d^0 \rightarrow \bar{K}_0^*(1430)^0 K^0), \quad (61)$$

$$\mathcal{A}(B^- \rightarrow K_0^*(1430)^0 K^-) \approx \mathcal{A}(\bar{B}_d^0 \rightarrow K_0^*(1430)^0 \bar{K}^0), \quad (62)$$

$$\mathcal{A}(B^- \rightarrow \bar{K}_0^*(1430)^0 \pi^-) \approx \mathcal{A}(\bar{B}_d^0 \rightarrow \bar{K}_0^*(1430)^0 \pi^0) \approx \mathcal{A}(\bar{B}_s^0 \rightarrow \bar{K}_0^*(1430)^0 K^0), \quad (63)$$

$$\mathcal{A}(B^- \rightarrow K_0^*(1430)^- \pi^0) \approx \mathcal{A}(B_d^0 \rightarrow K_0^*(1430)^- \pi^+) \approx \mathcal{A}(\bar{B}_s^0 \rightarrow K_0^*(1430)^- K^+), \quad (64)$$

which further imply that

$$R_1 \equiv \frac{\Gamma_{B^- \rightarrow K_0^*(1430)^- K^0}}{\Gamma_{\bar{B}_d^0 \rightarrow \bar{K}_0^*(1430)^0 K^0}} \approx 1, \quad R_2 \equiv \frac{\Gamma_{B^- \rightarrow K_0^*(1430)^0 K^-}}{\Gamma_{\bar{B}_d^0 \rightarrow K_0^*(1430)^0 \bar{K}^0}} \approx 1, \quad (65)$$

$$R_3 \equiv \frac{\Gamma_{B^- \rightarrow \bar{K}_0^*(1430)^0 \pi^-}}{2\Gamma_{\bar{B}_d^0 \rightarrow \bar{K}_0^*(1430)^0 \pi^0}} \approx 1, \quad R'_3 \equiv \frac{\Gamma_{B^- \rightarrow \bar{K}_0^*(1430)^0 \pi^-}}{\Gamma_{\bar{B}_s^0 \rightarrow \bar{K}_0^*(1430)^0 K^0}} \approx 1, \quad (66)$$

$$R_4 \equiv \frac{2\Gamma_{B^- \rightarrow K_0^*(1430)^- \pi^0}}{\Gamma_{B_d^0 \rightarrow K_0^*(1430)^- \pi^+}} \approx 1, \quad R'_4 \equiv \frac{2\Gamma_{B^- \rightarrow K_0^*(1430)^- \pi^0}}{\Gamma_{\bar{B}_s^0 \rightarrow K_0^*(1430)^- K^+}} \approx 1. \quad (67)$$

Besides, the $SU(3)$ flavor symmetry also expects that

$$R_5 \equiv \frac{\Gamma_{\bar{B}_d^0 \rightarrow K_0^*(1430)^- \pi^+}}{2\Gamma_{\bar{B}_d^0 \rightarrow \bar{K}_0^*(1430)^0 \pi^0}} \approx 1, \quad R_6 \equiv \frac{\Gamma_{B^- \rightarrow \bar{K}_0^*(1430)^0 \pi^-}}{2\Gamma_{B^- \rightarrow K_0^*(1430)^- \pi^0}} \approx 1. \quad (68)$$

It is found in our calculation (S2) that

$$R_1 = 0.93, \quad R_2 = 1.00, \quad R_3 = 1.12, \quad R'_3 = 1.10, \quad R_4 = 0.99, \quad R'_4 = 1.08, \quad (69)$$

$$R_5 = 1.11, \quad R_6 = 0.90, \quad (70)$$

which generally agree with the expectations of $SU(3)$ flavor symmetry. The flavor symmetry breaking effect is mainly ascribed to the remaining suppressed contributions. Taking

Table 9: The branching fractions (in units of 10^{-6}) of $\bar{B}_{d,s}^0 \rightarrow \bar{K}_0^*(1430)K^{(*)} + c.c.$ decays in S2.

Decay modes	this work	pQCD [45]	data
$\bar{B}_d^0 \rightarrow K_0^{*0} \bar{K}^0 + c.c.$	$3.05_{-0.13-0.59-1.29}^{+0.17+0.35+1.61}$		
$\bar{B}_d^0 \rightarrow K_0^{*+} K^- + c.c.$	$0.17_{-0.01-0.05-0.05}^{+0.01+0.03+0.07}$		
$\bar{B}_s^0 \rightarrow K_0^{*0} \bar{K}^0 + c.c.$	$32.78_{-1.02-7.08-13.39}^{+1.45+4.17+16.59}$		33.0 ± 10.1
$\bar{B}_s^0 \rightarrow K_0^{*+} K^- + c.c.$	$33.73_{-1.07-7.09-13.43}^{+1.51+4.17+16.65}$		31.3 ± 25.4
$\bar{B}_d^0 \rightarrow K_0^{*0} \bar{K}^{*0} + c.c.$	$2.52_{-0.11-0.49-1.03}^{+0.14+0.29+1.28}$	$0.59_{-0.1}^{+0.1}$	
$\bar{B}_d^0 \rightarrow K_0^{*+} K^{*-} + c.c.$	$0.07_{-0.00-0.01-0.02}^{+0.01+0.01+0.03}$	$1.1_{-0.1}^{+0.1}$	
$\bar{B}_s^0 \rightarrow K_0^{*0} \bar{K}^{*0} + c.c.$	$34.98_{-1.09-6.14-14.57}^{+1.55+3.56+18.02}$	$13.0_{-2.0}^{+2.0}$	
$\bar{B}_s^0 \rightarrow K_0^{*+} K^{*-} + c.c.$	$33.81_{-1.07-5.98-13.85}^{+1.51+3.47+17.13}$	$15.0_{-3.0}^{+4.0}$	

R_6 as an example, the amplitude of $B^- \rightarrow K_0^*(1430)^- \pi^0$ decay receives additional CKM-suppressed contributions proportional to $\delta_{pu}\alpha_1$, as well as CKM- and color-suppressed $\delta_{pu}\alpha_2$, compared with $B^- \rightarrow \bar{K}_0^*(1430)^0 \pi^-$ decay.

- The $\mathcal{O}(\alpha_s^2)$ corrections to the amplitudes of non-leptonic two-body B decays have been evaluated in recent years [119–129]. In Ref. [119], it is found that the next-to-next-to-leading order (NNLO) vertex correction to the color-suppressed amplitude α_2 is sizable, but when combined with the $\mathcal{O}(\alpha_s^2)$ correction to spectator scattering, the overall NNLO corrections to the color-allowed and -suppressed tree amplitudes are small due to the large cancellation. Therefore, the $\mathcal{O}(\alpha_s^2)$ corrections to the tree-dominated $\bar{B}_s^0 \rightarrow K_0^*(1430)^+ \pi^- / \rho^-$ and $\bar{B}_s^0 \rightarrow K_0^*(1430)^0 \pi^0 / \rho^0(\omega)$ decays would not be significant. The NNLO correction to the penguin amplitude has also been studied in Refs. [120, 121]. It is found that the NNLO contributions from current-current and penguin operators are sizable, but there is a strong cancellation between them, which results in a much reduced overall NNLO corrections to the penguin amplitude $a_4^{u,c}$. As a consequence the full NNLO result for $a_4^{u,c}$ is very close to the NLO result [121] (an example, $a_4^{u,c}(\pi \bar{K})$, is shown by Fig. 8 in Ref. [121]). Therefore, based on these previous works on the $\mathcal{O}(\alpha_s^2)$ correction, we can expect that the $\mathcal{O}(\alpha_s^2)$ corrections do not affect the main findings of this work.

Table 10: The CP asymmetry parameters (in units of 10^{-2}) of $\bar{B}_{d,s}^0 \rightarrow \bar{K}_0^*(1430)K^{(*)} + c.c.$ decays in S2.

	A_{CP}	C	ΔC	S	ΔS
$\bar{B}_d^0 \rightarrow \bar{K}_0^{*0}K^0 + c.c.$	$-20.24_{-0.75}^{+0.77}$	$10.04_{-0.38}^{+0.37}$	$-10.72_{-0.40}^{+0.41}$	$2.15_{-0.08}^{+0.08}$	$8.70_{-0.36}^{+0.36}$
$\bar{B}_d^0 \rightarrow K_0^{*-}K^+ + c.c.$	$1.42_{-0.05}^{+0.06}$	$-0.04_{-0.00}^{+0.00}$	$1.42_{-0.05}^{+0.05}$	$4.76_{-7.64}^{+8.13}$	$6.35_{-0.25}^{+0.22}$
$\bar{B}_s^0 \rightarrow \bar{K}_0^{*0}K^0 + c.c.$	$-0.74_{-0.02}^{+0.02}$	$-0.42_{-0.01}^{+0.01}$	$-0.40_{-0.01}^{+0.01}$	$0.03_{-0.00}^{+0.00}$	$0.31_{-0.01}^{+0.01}$
$\bar{B}_s^0 \rightarrow K_0^{*-}K^+ + c.c.$	$-8.56_{-0.26}^{+0.26}$	$31.27_{-0.78}^{+0.76}$	$-32.52_{-0.80}^{+0.82}$	$-11.39_{-0.56}^{+0.60}$	$3.49_{-0.54}^{+0.50}$
$\bar{B}_d^0 \rightarrow \bar{K}_0^{*0}K^{*0} + c.c.$	$-14.03_{-0.52}^{+0.53}$	$9.87_{-0.37}^{+0.36}$	$-5.91_{-0.22}^{+0.23}$	$-14.20_{-0.53}^{+0.54}$	$-6.58_{-0.23}^{+0.24}$
$\bar{B}_d^0 \rightarrow K_0^{*-}K^{*+} + c.c.$	$-0.52_{-0.02}^{+0.02}$	$4.69_{-0.18}^{+0.18}$	$0.42_{-0.02}^{+0.02}$	$5.61_{-7.67}^{+8.16}$	$-0.75_{-0.03}^{+0.03}$
$\bar{B}_s^0 \rightarrow \bar{K}_0^{*0}K^{*0} + c.c.$	$-0.55_{-0.02}^{+0.02}$	$-0.44_{-0.01}^{+0.01}$	$-0.24_{-0.01}^{+0.01}$	$0.70_{-0.02}^{+0.02}$	$-0.23_{-0.01}^{+0.01}$
$\bar{B}_s^0 \rightarrow K_0^{*-}K^{*+} + c.c.$	$-7.74_{-0.23}^{+0.23}$	$22.86_{-0.77}^{+0.74}$	$-23.27_{-0.75}^{+0.77}$	$30.72_{-0.71}^{+0.69}$	$-23.55_{-0.47}^{+0.49}$

Different from the other decay modes, \bar{B}_s^0 or \bar{B}_d^0 can decay into $\bar{K}_0^*(1430)K^{(*)}$ and its CP conjugate state simultaneously. The sum of the $\bar{K}_0^*(1430)K^{(*)}$ and $K_0^*(1430)\bar{K}^{(*)}$ decay rates is measured more accurately than the individual rates. Our prediction for $\bar{B}_{d,s}^0 \rightarrow \bar{K}_0^*(1430)K^{(*)} + c.c.$ decays are given in table 9, the LHCb data [21] given by Eq. (1) and the pQCD predictions [45] are also listed for comparison. In addition, the CP violations of $\bar{B}_{d,s}^0 \rightarrow \bar{K}_0^*(1430)K^{(*)} + c.c.$ decays are much more complicated because $\bar{K}_0^*(1430)K^{(*)} + c.c.$ are not CP eigenstates. The system of these decays define five CP asymmetry parameters, C , ΔC , S , ΔS and A_{CP} , where S is referred to as mixing-induced CP asymmetry, C is the direct CP asymmetry, ΔC and ΔS are CP conserving quantities, and A_{CP} is the time-integrated charge asymmetry. Our results for these observables are first given in table 10.

The $\bar{B}_d^0 \rightarrow K_0^{*-}K^{(*)+} + c.c.$ decays are caused by the pure annihilation transition, and therefore have very small branching fractions $\sim \mathcal{O}(10^{-7})$. The $\bar{B}_d^0 \rightarrow \bar{K}_0^{*0}K^{(*)0} + c.c.$ decays are dominated by penguin contributions, but are CKM-suppressed. The penguin-dominated $\bar{B}_s^0 \rightarrow K_0^{*-}K^{(*)+} + c.c.$ and $\bar{K}_0^{*0}K^{(*)0} + c.c.$ decays have relatively large branching fractions, and our results for the SP modes are in good agreement with the data obtained by the LHCb collaboration with significance over 10 standard deviations [21]. However, some systematic variations do impact strongly on the need to include tensor resonances in the fit model, and thus the model uncertainties of experimental data are very large [21]. It is expected that the

future refined measurements for the $\bar{B}_{d,s}^0 \rightarrow \bar{K}_0^*(1430)K^{(*)} + c.c.$ decays can provide serious test on the theoretical predictions.

4 Summary

In this paper, the nonleptonic charmless $B_{u,d,s} \rightarrow K_0^*(1430)P$ ($P = K, \pi$) and $K_0^*(1430)V$ ($V = K^*, \rho, \omega, \phi$) decays are studied. The amplitudes are calculated by using the QCD factorization approach, and the non-perturbative quantities (form factor, decay constant and distribution amplitudes) are evaluated by using a covariant light-front approach. The branching fractions and CP asymmetries of these decay modes are calculated, our main theoretical results are collected in tables 5-10. Some decay modes are first predicted in this work. In order to test the underlying structure of $K_0^*(1430)$ meson, our calculation are made based on two different scenarios that $K_0^*(1430)$ is the first excited (scenario S1) and the lowest-lying (scenario S2) p-wave two-quark state. Comparing our results with data, we find that the scenarios S1 and S2 lead to significantly different results for branching fractions, and the results based on scenario S2 agree well with the experimental data, which implies that $K_0^*(1430)$ as the lowest-lying (scenario S2) p-wave ($s, u/d$) state is favored by data. However, the theoretical results for $\mathcal{B}(B^- \rightarrow K_0^*(1430)^0 K^-)$ are much larger than data due to the large chiral factor $\gamma_X^{K_0^{*0}}$. The future refined measurement on $\mathcal{B}(B^- \rightarrow K_0^*(1430)^0 K^-)$ is required for confirming or refuting such possible anomaly. Besides, some useful relations based on $SU(3)$ flavor symmetry are studied.

Acknowledgements

This work is supported by the National Natural Science Foundation of China (Grant No. 11875122), Excellent Youth Foundation of Henan Province (Grant No. 212300410010), The Youth Talent Support Program of Henan Province (Grant No. ZYQR201912178) and the Program for Innovative Research Team in University of Henan Province (Grant No. 19IRT-STHN018).

Appendix A: Decay constant, form factor and DAs

The decay constant, form factor and DAs are essential nonperturbative inputs for the amplitudes of $B \rightarrow SP$ and SV . In this sections, we would like to clarify our convention for the definitions of these nonperturbative quantities.

A.1 Decay constant

The decay constants of pseudoscalar (P), vector (V) and scalar (S) mesons are defined as

$$\begin{aligned}\langle P(p) | \bar{q}_1 \gamma^\mu \gamma^5 q_2 | 0 \rangle &= -i f_P p_\mu, & \langle V(p, \epsilon) | \bar{q}_1 \gamma^\mu q_2 | 0 \rangle &= -i f_V m_V \epsilon^{*\mu}, \\ \langle S(p) | \bar{q}_1 \gamma^\mu q_2 | 0 \rangle &= f_S p_\mu, & \langle S(p) | \bar{q}_1 q_2 | 0 \rangle &= m_S \bar{f}_S(\mu).\end{aligned}\quad (71)$$

The scale-dependent scalar decay constant $\bar{f}_S(\mu)$ and the vector decay constant f_S are related by the equation of motion, and thus have the following relation,

$$\bar{f}_S = \frac{\mu_S}{m_S} f_S \equiv \bar{\mu}_S f_S, \quad \text{with} \quad \mu_S = \frac{m_S^2}{m_1(\mu) - m_2(\mu)}, \quad (72)$$

where $m_1(\mu)$ and $m_2(\mu)$ are running masses of current quarks.

A.2 Form factor

The form factors of $B \rightarrow S, P, V$ transitions concerned in this paper can be defined as

$$\langle S(p'') | \bar{q} \gamma_\mu \gamma_5 b | B(p') \rangle = -i \left[\left(P_\mu - \frac{m_B^2 - m_S^2}{q^2} q_\mu \right) U_1(q^2) + \frac{m_B^2 - m_S^2}{q^2} q_\mu U_0(q^2) \right], \quad (73)$$

$$\langle P(p'') | \bar{q} \gamma_\mu b | B(p') \rangle = \left(P_\mu - \frac{m_B^2 - m_P^2}{q^2} q_\mu \right) F_1(q^2) + \frac{m_B^2 - m_P^2}{q^2} q_\mu F_0(q^2), \quad (74)$$

$$\langle V(\epsilon, p'') | \bar{q} \gamma_\mu b | B(p') \rangle = -i \frac{V(q^2)}{m_B + m_V} \varepsilon_{\mu\nu\alpha\beta} \epsilon^{*\nu} P^\alpha q^\beta, \quad (75)$$

$$\begin{aligned}\langle V(\epsilon, p'') | \bar{q} \gamma_\mu \gamma_5 b | B(p') \rangle &= 2m_V \frac{\epsilon^* \cdot P}{q^2} q_\mu A_0(q^2) + (m_B + m_V) \left(\epsilon_\mu^* - \frac{\epsilon^* \cdot P}{q^2} q_\mu \right) A_1(q^2) \\ &\quad - \frac{\epsilon^* \cdot P}{m_B + m_V} \left(P_\mu - \frac{m_B^2 - m_V^2}{q^2} q_\mu \right) A_2(q^2),\end{aligned}\quad (76)$$

where $P_\mu = (p' + p'')$, $q_\mu = (p' - p'')$ and $\varepsilon_{0123} = -1$. The momentum dependence of form factor can be parameterized as

$$F(q^2) = \frac{F(0)}{1 - a(q^2/m_B^2) + b(q^2/m_B^2)^2}. \quad (77)$$

The values of parameters a , b and $F(0)$ for the transition concerned in this work are summarized in Table 1.

A.2 Distribution amplitude

For the light-cone distribution amplitudes of pseudoscalar and vector mesons, we take the same definition and convention used in the Ref. [70]. For the scalar meson, the twist-2 and -3 light-cone distribution amplitudes are given by

$$\langle S(p) | \bar{q}_2(z_2) \gamma_\mu q_1(z_1) | 0 \rangle = f_S p_\mu \int_0^1 dx e^{i(xp \cdot z_2 + \bar{x}p \cdot z_1)} \Phi_S(x), \quad (78)$$

$$\langle S(p) | \bar{q}_2(z_2) q_1(z_1) | 0 \rangle = f_S \mu_S \int_0^1 dx e^{i(xp \cdot z_2 + \bar{x}p \cdot z_1)} \phi_S(x), \quad (79)$$

$$\langle S(p) | \bar{q}_2(z_2) \sigma_{\mu\nu} q_1(z_1) | 0 \rangle = -f_S \mu_S (p_\mu z_\nu - p_\nu z_\mu) \int_0^1 dx e^{i(xp \cdot z_2 + \bar{x}p \cdot z_1)} \frac{\phi_S^\sigma(x)}{6}. \quad (80)$$

The leading-twist DAs are conventionally expanded in Gegenbauer polynomials,

$$\Phi_M(x, \mu) = 6x(1-x) \left[1 + \sum_{n=1}^{\infty} a_n^M(\mu) C_n^{3/2}(x-\bar{x}) \right], \quad (81)$$

where $M = P, S, V$. Equivalently, for the scalar meson, one can also use

$$\Phi_S(x) = 6x(1-x) \bar{\mu}_S(\mu) \left[b_0^S + \sum_{n=1}^{\infty} b_n^S(\mu) C_n^{3/2}(x-\bar{x}) \right], \quad (82)$$

where, $a_n^S(\mu) = \bar{\mu}_S(\mu) b_n^S(\mu)$ and $\bar{\mu}_S(\mu)$ can be conveniently absorbed by f_S via Eq. (72).

When three-particle contributions are neglected, the twist-3 two-particle DAs of P and S mesons are determined completely by the equation of motion, which then require

$$\phi_{P,S} = 1, \quad \phi_{P,S}^\sigma = 6x\bar{x}; \quad (83)$$

For the vector meson, the twist-3 DAs can be expressed in terms of the leading-twist DA $\Phi_\perp(x)$ of transversely polarized state, are usually expressed by the function, ϕ_V , defined as

$$\phi_V(x, \mu) \equiv \int_0^x dv \frac{\Phi_\perp(v)}{\bar{v}} - \int_x^1 dv \frac{\Phi_\perp(v)}{v} = 3 \sum_{n=0}^{\infty} a_{n,\perp}^V(\mu) P_{n+1}(2x-1), \quad (84)$$

where $a_{0,\perp}^V = 1$ and $P_n(x)$ are the Legendre polynomials.

Appendix B: Decay amplitudes

The amplitudes of $B_{u,d,s} \rightarrow K_0^*(1430)P$ ($P = K, \pi$) decays are written as

$$\mathcal{A}_{B^- \rightarrow K_0^{*-} K^0} = A_{K_0^* K} [\delta_{pu} \beta_2 + \alpha_4^p - \frac{1}{2} \alpha_{4,EW}^p + \beta_3^p + \beta_{3,EW}^p], \quad (85)$$

$$\mathcal{A}_{B^- \rightarrow K_0^{*0} K^-} = A_{K K_0^*} [\delta_{pu} \beta_2 + \alpha_4^p - \frac{1}{2} \alpha_{4,EW}^p + \beta_3^p + \beta_{3,EW}^p], \quad (86)$$

$$\mathcal{A}_{B^- \rightarrow \bar{K}_0^{*0} \pi^-} = A_{\pi K_0^*} [\delta_{pu} \beta_2 + \alpha_4^p - \frac{1}{2} \alpha_{4,EW}^p + \beta_3^p + \beta_{3,EW}^p], \quad (87)$$

$$\begin{aligned} \mathcal{A}_{B^- \rightarrow K_0^{*-} \pi^0} &= \frac{1}{\sqrt{2}} A_{\pi K_0^*} [\delta_{pu} (\alpha_1 + \beta_2) + \alpha_4^p + \alpha_{4,EW}^p + \beta_3^p + \beta_{3,EW}^p] \\ &\quad + \frac{1}{\sqrt{2}} A_{K_0^* \pi} [\delta_{pu} \alpha_2 + \frac{3}{2} \alpha_{3,EW}^p], \end{aligned} \quad (88)$$

$$\begin{aligned} \mathcal{A}_{\bar{B}^0 \rightarrow \bar{K}_0^{*0} K^0} &= A_{K_0^* K} [\alpha_4^p - \frac{1}{2} \alpha_{4,EW}^p + \beta_3^p + \beta_4^p - \frac{1}{2} \beta_{3,EW}^p - \frac{1}{2} \beta_{4,EW}^p] \\ &\quad + B_{K K_0^*} [b_4^p - \frac{1}{2} b_{4,EW}^p], \end{aligned} \quad (89)$$

$$\begin{aligned} \mathcal{A}_{\bar{B}^0 \rightarrow K_0^{*0} \bar{K}^0} &= A_{K K_0^*} [\alpha_4^p - \frac{1}{2} \alpha_{4,EW}^p + \beta_3^p + \beta_4^p - \frac{1}{2} \beta_{3,EW}^p - \frac{1}{2} \beta_{4,EW}^p] \\ &\quad + B_{K_0^* K} [b_4^p - \frac{1}{2} b_{4,EW}^p], \end{aligned} \quad (90)$$

$$\mathcal{A}_{\bar{B}^0 \rightarrow K_0^{*-} K^+} = A_{K_0^* K} [\delta_{pu} \beta_1 + \beta_4^p + \beta_{4,EW}^p] + B_{K K_0^*} [b_4^p - \frac{1}{2} b_{4,EW}^p], \quad (91)$$

$$\mathcal{A}_{\bar{B}^0 \rightarrow K_0^{*+} K^-} = A_{K K_0^*} [\delta_{pu} \beta_1 + \beta_4^p + \beta_{4,EW}^p] + B_{K_0^* K} [b_4^p - \frac{1}{2} b_{4,EW}^p], \quad (92)$$

$$\mathcal{A}_{\bar{B}^0 \rightarrow K_0^{*+} \pi^-} = A_{\pi K_0^*} [\delta_{pu} \alpha_1 + \alpha_4^p + \alpha_{4,EW}^p + \beta_3^p - \frac{1}{2} \beta_{3,EW}^p], \quad (93)$$

$$\begin{aligned} \mathcal{A}_{\bar{B}^0 \rightarrow \bar{K}_0^{*0} \pi^0} &= \frac{1}{\sqrt{2}} A_{\pi K_0^*} [-\alpha_4^p + \frac{1}{2} \alpha_{4,EW}^p - \beta_3^p + \frac{1}{2} \beta_{3,EW}^p] \\ &\quad + \frac{1}{\sqrt{2}} A_{K_0^* \pi} [\delta_{pu} \alpha_2 + \frac{3}{2} \alpha_{3,EW}^p], \end{aligned} \quad (94)$$

$$\begin{aligned} \mathcal{A}_{\bar{B}_s^0 \rightarrow \bar{K}_0^{*0} K^0} &= A_{K K_0^*} [\alpha_4^p - \frac{1}{2} \alpha_{4,EW}^p + \beta_3^p + \beta_4^p - \frac{1}{2} \beta_{3,EW}^p - \frac{1}{2} \beta_{4,EW}^p] \\ &\quad + B_{K_0^* K} [b_4^p - \frac{1}{2} b_{4,EW}^p], \end{aligned} \quad (95)$$

$$\begin{aligned} \mathcal{A}_{\bar{B}_s^0 \rightarrow K_0^{*0} \bar{K}^0} &= A_{K_0^* K} [\alpha_4^p - \frac{1}{2} \alpha_{4,EW}^p + \beta_3^p + \beta_4^p - \frac{1}{2} \beta_{3,EW}^p - \frac{1}{2} \beta_{4,EW}^p] \\ &\quad + B_{K K_0^*} [b_4^p - \frac{1}{2} b_{4,EW}^p], \end{aligned} \quad (96)$$

$$\begin{aligned} \mathcal{A}_{\bar{B}_s^0 \rightarrow K_0^{*-} K^+} &= A_{K K_0^*} [\delta_{pu} \alpha_1 + \alpha_4^p + \alpha_{4,EW}^p + \beta_3^p + \beta_4^p - \frac{1}{2} \beta_{3,EW}^p - \frac{1}{2} \beta_{4,EW}^p] \\ &\quad + B_{K_0^* K} [\delta_{pu} b_1 + b_4^p + b_{4,EW}^p], \end{aligned} \quad (97)$$

$$\begin{aligned}\mathcal{A}_{\bar{B}_s^0 \rightarrow K_0^{*+} K^-} &= A_{K_0^* K} [\delta_{pu} \alpha_1 + \alpha_4^p + \alpha_{4,EW}^p + \beta_3^p + \beta_4^p - \frac{1}{2} \beta_{3,EW}^p - \frac{1}{2} \beta_{4,EW}^p] \\ &\quad + B_{K K_0^*} [\delta_{pu} b_1 + b_4^p + b_{4,EW}^p],\end{aligned}\quad (98)$$

$$\mathcal{A}_{\bar{B}_s^0 \rightarrow K_0^{*+} \pi^-} = A_{K_0^* \pi} [\delta_{pu} \alpha_1 + \alpha_4^p + \alpha_{4,EW}^p + \beta_3^p - \frac{1}{2} \beta_{3,EW}^p], \quad (99)$$

$$\mathcal{A}_{\bar{B}_s^0 \rightarrow K_0^{*0} \pi^0} = \frac{1}{\sqrt{2}} A_{K_0^* \pi} [\delta_{pu} \alpha_2 - \alpha_4^p + \frac{3}{2} \alpha_{3,EW}^p + \frac{1}{2} \alpha_{4,EW}^p - \beta_3^p + \frac{1}{2} \beta_{3,EW}^p]. \quad (100)$$

The amplitudes of $B_{u,d,s} \rightarrow K_0^*(1430)V$ ($V = \rho, K^*, \omega, \phi$) decays are written as

$$\mathcal{A}_{B^- \rightarrow K_0^{*-} K^{*0}} = A_{K_0^* K^*} [\delta_{pu} \beta_2 + \alpha_4^p - \frac{1}{2} \alpha_{4,EW}^p + \beta_3^p + \beta_{3,EW}^p], \quad (101)$$

$$\mathcal{A}_{B^- \rightarrow K_0^{*0} K^{*-}} = A_{K^* K_0^*} [\delta_{pu} \beta_2 + \alpha_4^p - \frac{1}{2} \alpha_{4,EW}^p + \beta_3^p + \beta_{3,EW}^p], \quad (102)$$

$$\mathcal{A}_{B^- \rightarrow \bar{K}_0^{*0} \rho^-} = A_{\rho K_0^*} [\delta_{pu} \beta_2 + \alpha_4^p - \frac{1}{2} \alpha_{4,EW}^p + \beta_3^p + \beta_{3,EW}^p], \quad (103)$$

$$\begin{aligned}\mathcal{A}_{B^- \rightarrow K_0^{*-} \rho^0} &= \frac{1}{\sqrt{2}} A_{\rho K_0^*} [\delta_{pu} (\alpha_1 + \beta_2) + \alpha_4^p + \alpha_{4,EW}^p + \beta_3^p + \beta_{3,EW}^p] \\ &\quad + \frac{1}{\sqrt{2}} A_{K_0^* \rho} [\delta_{pu} \alpha_2 + \frac{3}{2} \alpha_{3,EW}^p],\end{aligned}\quad (104)$$

$$\begin{aligned}\mathcal{A}_{B^- \rightarrow K_0^{*-} \omega} &= \frac{1}{\sqrt{2}} A_{\omega K_0^*} [\delta_{pu} (\alpha_1 + \beta_2) + \alpha_4^p + \alpha_{4,EW}^p + \beta_3^p + \beta_{3,EW}^p] \\ &\quad + \frac{1}{\sqrt{2}} A_{K_0^* \omega} [\delta_{pu} \alpha_2 + 2\alpha_3^p + \frac{1}{2} \alpha_{3,EW}^p],\end{aligned}\quad (105)$$

$$\mathcal{A}_{B^- \rightarrow K_0^{*-} \phi} = A_{K_0^* \phi} [\delta_{pu} \beta_2 + \alpha_3^p + \alpha_4^p - \frac{1}{2} \alpha_{3,EW}^p - \frac{1}{2} \alpha_{4,EW}^p + \beta_3^p + \beta_{3,EW}^p], \quad (106)$$

$$\begin{aligned}\mathcal{A}_{\bar{B}^0 \rightarrow \bar{K}_0^{*0} K^{*0}} &= A_{K_0^* K^*} [\alpha_4^p - \frac{1}{2} \alpha_{4,EW}^p + \beta_3^p + \beta_4^p - \frac{1}{2} \beta_{3,EW}^p - \frac{1}{2} \beta_{4,EW}^p] \\ &\quad + B_{K^* K_0^*} [b_4^p - \frac{1}{2} b_{4,EW}^p],\end{aligned}\quad (107)$$

$$\begin{aligned}\mathcal{A}_{\bar{B}^0 \rightarrow K_0^{*0} \bar{K}^{*0}} &= A_{K^* K_0^*} [\alpha_4^p - \frac{1}{2} \alpha_{4,EW}^p + \beta_3^p + \beta_4^p - \frac{1}{2} \beta_{3,EW}^p - \frac{1}{2} \beta_{4,EW}^p] \\ &\quad + B_{K_0^* K^*} [b_4^p - \frac{1}{2} b_{4,EW}^p],\end{aligned}\quad (108)$$

$$\mathcal{A}_{\bar{B}^0 \rightarrow K_0^{*-} K^{*+}} = A_{K_0^* K^*} [\delta_{pu} \beta_1 + \beta_4^p + \beta_{4,EW}^p] + B_{K^* K_0^*} [b_4^p - \frac{1}{2} b_{4,EW}^p], \quad (109)$$

$$\mathcal{A}_{\bar{B}^0 \rightarrow K_0^{*+} K^{*-}} = A_{K^* K_0^*} [\delta_{pu} \beta_1 + \beta_4^p + \beta_{4,EW}^p] + B_{K_0^* K^*} [b_4^p - \frac{1}{2} b_{4,EW}^p], \quad (110)$$

$$\mathcal{A}_{\bar{B}^0 \rightarrow K_0^{*-} \rho^+} = A_{\rho K_0^*} [\delta_{pu} \alpha_1 + \alpha_4^p + \alpha_{4,EW}^p + \beta_3^p - \frac{1}{2} \beta_{3,EW}^p], \quad (111)$$

$$\begin{aligned}\mathcal{A}_{\bar{B}^0 \rightarrow \bar{K}_0^{*0} \rho^0} &= \frac{1}{\sqrt{2}} A_{\rho K_0^*} [-\alpha_4^p + \frac{1}{2} \alpha_{4,EW}^p - \beta_3^p + \frac{1}{2} \beta_{3,EW}^p] \\ &\quad + \frac{1}{\sqrt{2}} A_{K_0^* \rho} [\delta_{pu} \alpha_2 + \frac{3}{2} \alpha_{3,EW}^p],\end{aligned}\quad (112)$$

$$\begin{aligned}\mathcal{A}_{\bar{B}^0 \rightarrow \bar{K}_0^{*0} \omega} &= \frac{1}{\sqrt{2}} A_{\omega K_0^*} [\alpha_4^p - \frac{1}{2} \alpha_{4,EW}^p + \beta_3^p - \frac{1}{2} \beta_{3,EW}^p] \\ &\quad + \frac{1}{\sqrt{2}} A_{K_0^* \omega} [\delta_{pu} \alpha_2 + 2\alpha_3^p + \frac{1}{2} \alpha_{3,EW}^p],\end{aligned}\tag{113}$$

$$\mathcal{A}_{\bar{B}^0 \rightarrow \bar{K}_0^{*0} \phi} = A_{K_0^* \phi} [\alpha_3^p + \alpha_4^p - \frac{1}{2} \alpha_{3,EW}^p - \frac{1}{2} \alpha_{4,EW}^p + \beta_3^p - \frac{1}{2} \beta_{3,EW}^p],\tag{114}$$

$$\begin{aligned}\mathcal{A}_{\bar{B}_s^0 \rightarrow \bar{K}_0^{*0} K^{*0}} &= A_{K^* K_0^*} [\alpha_4^p - \frac{1}{2} \alpha_{4,EW}^p + \beta_3^p + \beta_4^p - \frac{1}{2} \beta_{3,EW}^p - \frac{1}{2} \beta_{4,EW}^p] \\ &\quad + B_{K_0^* K^*} [b_4^p - \frac{1}{2} b_{4,EW}^p],\end{aligned}\tag{115}$$

$$\begin{aligned}\mathcal{A}_{\bar{B}_s^0 \rightarrow K_0^{*0} \bar{K}^{*0}} &= A_{K_0^* K^*} [\alpha_4^p - \frac{1}{2} \alpha_{4,EW}^p + \beta_3^p + \beta_4^p - \frac{1}{2} \beta_{3,EW}^p - \frac{1}{2} \beta_{4,EW}^p] \\ &\quad + B_{K^* K_0^*} [b_4^p - \frac{1}{2} b_{4,EW}^p],\end{aligned}\tag{116}$$

$$\begin{aligned}\mathcal{A}_{\bar{B}_s^0 \rightarrow K_0^{*-} K^{*+}} &= A_{K^* K_0^*} [\delta_{pu} \alpha_1 + \alpha_4^p + \alpha_{4,EW}^p + \beta_3^p + \beta_4^p - \frac{1}{2} \beta_{3,EW}^p - \frac{1}{2} \beta_{4,EW}^p] \\ &\quad + B_{K_0^* K^*} [\delta_{pu} b_1 + b_4^p + b_{4,EW}^p],\end{aligned}\tag{117}$$

$$\begin{aligned}\mathcal{A}_{\bar{B}_s^0 \rightarrow K_0^{*+} K^{*-}} &= A_{K_0^* K^*} [\delta_{pu} \alpha_1 + \alpha_4^p + \alpha_{4,EW}^p + \beta_3^p + \beta_4^p - \frac{1}{2} \beta_{3,EW}^p - \frac{1}{2} \beta_{4,EW}^p] \\ &\quad + B_{K^* K_0^*} [\delta_{pu} b_1 + b_4^p + b_{4,EW}^p],\end{aligned}\tag{118}$$

$$\mathcal{A}_{\bar{B}_s \rightarrow K_0^{*+} \rho^-} = A_{K_0^* \rho} [\delta_{pu} \alpha_1 + \alpha_4^p + \alpha_{4,EW}^p + \beta_3^p - \frac{1}{2} \beta_{3,EW}^p],\tag{119}$$

$$\mathcal{A}_{\bar{B}_s \rightarrow K_0^{*0} \rho^0} = \frac{1}{\sqrt{2}} A_{K_0^* \rho} [\delta_{pu} \alpha_2 - \alpha_4^p + \frac{3}{2} \alpha_{3,EW}^p + \frac{1}{2} \alpha_{4,EW}^p - \beta_3^p + \frac{1}{2} \beta_{3,EW}^p],\tag{120}$$

$$\mathcal{A}_{\bar{B}_s \rightarrow K_0^{*0} \omega} = \frac{1}{\sqrt{2}} A_{K_0^* \omega} [\delta_{pu} \alpha_2 + 2\alpha_3^p + \alpha_4^p + \frac{1}{2} \alpha_{3,EW}^p - \frac{1}{2} \alpha_{4,EW}^p + \beta_3^p - \frac{1}{2} \beta_{3,EW}^p],\tag{121}$$

$$\mathcal{A}_{\bar{B}_s \rightarrow K_0^{*0} \phi} = A_{\phi K_0^*} [\alpha_4^p - \frac{1}{2} \alpha_{4,EW}^p + \beta_3^p - \frac{1}{2} \beta_{3,EW}^p] + A_{K_0^* \phi} [\alpha_3^p - \frac{1}{2} \alpha_{3,EW}^p].\tag{122}$$

References

- [1] R. L. Jaffe, Phys. Rev. D **15** (1977) 267.
- [2] R. L. Jaffe, Phys. Rev. D **15** (1977) 281.
- [3] N. Mathur *et al.*, Phys. Rev. D **76** (2007) 114505.
- [4] S. Prelovsek, T. Draper, C. B. Lang, M. Limmer, K. F. Liu, N. Mathur and D. Mohler, Phys. Rev. D **82** (2010) 094507.
- [5] F. E. Close and N. A. Tornqvist, J. Phys. G **28** (2002) R249.

- [6] K. Abe *et al.* [Belle Collaboration], Phys. Rev. D **65** (2002) 092005.
- [7] B. Aubert *et al.* [BaBar Collaboration], Phys. Rev. D **70** (2004) 092001.
- [8] T. Abe *et al.* [Belle Collaboration], Phys. Rev. Lett. **96** (2006) 251803.
- [9] P. Chang *et al.* [Belle Collaboration], Phys. Lett. B **599** (2004) 148.
- [10] M. Prim *et al.* [Belle Collaboration], Phys. Rev. D **88** (2013) no.7, 072004.
- [11] M. Prim *et al.* [Belle Collaboration], Phys. Rev. D **81** (2010) 071101.
- [12] J. P. Lees *et al.* [BABAR Collaboration], Phys. Rev. D **85** (2012) 112010.
- [13] J. P. Lees *et al.* [BABAR Collaboration], Phys. Rev. D **83** (2011) 112010.
- [14] B. Aubert *et al.* [BaBar Collaboration], Phys. Rev. D **79** (2009) 052005.
- [15] B. Aubert *et al.* [BaBar Collaboration], Phys. Rev. D **78** (2008) 012004.
- [16] B. Aubert *et al.* [BaBar Collaboration], Phys. Rev. Lett. **101** (2008) 161801.
- [17] B. Aubert *et al.* [BaBar Collaboration], Phys. Rev. D **78** (2008) 092008.
- [18] J. P. Lee *et al.* [BaBar Collaboration], Phys. Rev. D **85** (2012) 072005.
- [19] B. Aubert *et al.* [BaBar Collaboration], Phys. Rev. D **76** (2007) 071103.
- [20] J. P. Lees *et al.* [BaBar Collaboration], Phys. Rev. D **83** (2011) 112010.
- [21] R. Aaij *et al.* [LHCb Collaboration], JHEP **1906** (2019) 114.
- [22] R. Aaij *et al.* [LHCb Collaboration], JHEP **1907** (2019) 032.
- [23] H. Y. Cheng and C. K. Chua, Phys. Rev. D **102** (2020) no.5, 053006.
- [24] H. Y. Cheng, C. K. Chua and Z. Q. Zhang, Phys. Rev. D **94** (2016) no.9, 094015.
- [25] H. Y. Cheng and C. K. Chua, Phys. Rev. D **89** (2014) no.7, 074025.
- [26] H. Y. Cheng and C. K. Chua, Phys. Rev. D **88** (2013) 114014.

- [27] H. Y. Cheng, C. K. Chua and A. Soni, Phys. Rev. D **76** (2007) 094006.
- [28] B. El-Bennich, A. Furman, R. Kaminski, L. Lesniak, B. Loiseau and B. Moussallam, Phys. Rev. D **79** (2009) 094005.
- [29] Y. Li, H. Y. Zhang, Y. Xing, Z. H. Li and C. D. Lu, Phys. Rev. D **91** (2015) no.7, 074022.
- [30] H. Y. Cheng, C. K. Chua and K. C. Yang, Phys. Rev. D **73** (2006) 014017.
- [31] H. Y. Cheng, C. K. Chua and K. C. Yang, Phys. Rev. D **77** (2008) 014034.
- [32] H. Y. Cheng and C. K. Chua, Phys. Rev. D **82** (2010) 034014.
- [33] H. Y. Cheng, C. K. Chua, K. C. Yang and Z. Q. Zhang, Phys. Rev. D **87** (2013) no.11, 114001.
- [34] J. J. Qi, X. H. Guo, Z. Y. Wang, Z. H. Zhang and C. Wang, Phys. Rev. D **99** (2019) 076010.
- [35] N. Wang, Q. Chang, Y. L. Yang and J. F. Sun, J. Phys. G **46** (2019) no.9, 095001.
- [36] Z. T. Zou, Y. Li and X. Liu, Eur. Phys. J. C **80** (2020) no.6, 517.
- [37] Z. T. Zou, Y. Li and Q. X. Li, Eur. Phys. J. C **80** (2020) no.5, 394.
- [38] Z. T. Zou, Y. Li and X. Liu, Eur. Phys. J. C **77** (2017) no.12, 870.
- [39] Q. X. Li, L. Yang, Z. T. Zou, Y. Li and X. Liu, Eur. Phys. J. C **79** (2019) no.11, 960.
- [40] W. F. Wang, H. C. Hu, H. N. Li and C. D. Lu, Phys. Rev. D **89** (2014) no.7, 074031.
- [41] Z. Rui and W. F. Wang, Phys. Rev. D **97** (2018) no.3, 033006.
- [42] Z. Rui, Y. Q. Li and J. Zhang, Phys. Rev. D **99** (2019) no.9, 093007.
- [43] X. Liu, Z. Q. Zhang, Z. J. Xiao, Chin. Phys. C **34** (2010) 157.
- [44] X. Liu, Z. J. Xiao and Z. T. Zou, J. Phys. G **40** (2013) 025002.
- [45] X. Liu, Z. J. Xiao and Z. T. Zou, Phys. Rev. D **88** (2013) 094003.

- [46] R. H. Li, C. D. Lu, W. Wang and X. X. Wang, Phys. Rev. D **79** (2009) 014013.
- [47] Q. X. Li, L. Yang, Z. T. Zou, Y. Li and X. Liu, Eur. Phys. J. C **79** (2019) no.11, 960.
- [48] Z. T. Zou, Y. Li and X. liu, Phys. Rev. D **95** (2017) no.1, 016011.
- [49] Z. T. Zou, Y. Li and X. Liu, Eur. Phys. J. C **77** (2017) no.12, 870.
- [50] Z. Q. Zhang, S. J. Wang, L. Y. Zhang, Chin. Phys. C **37** (2013) 043103.
- [51] Z. Q. Zhang, EPL **97** (2012) no.1, 11001.
- [52] Z. Q. Zhang, Phys. Rev. D **82** (2010) 034036.
- [53] Z. Q. Zhang, Phys. Rev. D **82** (2010) 114016.
- [54] Z. W. Liu, Z. T. Zou, Y. Li, X. Liu and J. Wang, [arXiv:2111.04235 [hep-ph]].
- [55] B. El-Bennich, A. Furman, R. Kaminski, L. Lesniak and B. Loiseau, Phys. Rev. D **74** (2006) 114009.
- [56] H. Y. Cheng, C. K. Chua and C. W. Hwang, Phys. Rev. D **69** (2004) 074025.
- [57] X. W. Kang, T. Luo, Y. zhang, L. Y. Dai and C. Wang, Eur. Phys. J. C **78** (2018) no.11, 909.
- [58] A. Issadykov, M. A. Ivanov and S. K. Sakhiyev, Phys. Rev. D **91** (2015) no.7, 074007.
- [59] S. Cheng and J. M. Shen, Eur. Phys. J. C **80** (2020) no.6, 554.
- [60] Y. Li, E. L. Wang and H. Y. Zhang, Adv. High Energy Phys. **2013** (2013) 175287.
- [61] Y. Li, D. D. Wang and C. D. Lu, Chin. Phys. C **40** (2016) no.1, 013101.
- [62] N. Ghahramany and R. Khosravi, Phys. Rev. D **80** (2009) 016009.
- [63] T. M. Aliev, K. Azizi and M. Savci, Phys. Rev. D **76** (2007) 074017.
- [64] M. Z. Yang, Phys. Rev. D **73** (2006) 034027.
- [65] H. Y. Han, X. G. Wu, H. B. Fu, Q. L. Zhang and T. Zhong, Eur. Phys. J. A **49** (2013) 78.

- [66] Z. G. Wang, Eur. Phys. J. C **75** (2015) no.2, 50.
- [67] G. Buchalla, A. J. Buras, and M. E. Lautenbacher, Rev. Mod. Phys. **68** (1996) 1125.
- [68] M. Beneke, G. Buchalla, M. Neubert and C. T. Sachrajda, Phys. Rev. Lett. **83** (1999) 1914.
- [69] M. Beneke G. Buchalla, M. Neubert and C. T. Sachrajda, Nucl. Phys. B **606** (2001) 245.
- [70] M. Beneke and M. Neubert, Nucl. Phys. B **675** (2003) 333.
- [71] H. Y. Cheng, C. K. Chua, Phys. Rev. D **80** (2009) 114008.
- [72] H. Y. Cheng, C. K. Chua, Phys. Rev. D **80** (2009) 114026.
- [73] Q. Chang, J. F. Sun, Y. L. Yang, and X. N. Li Phys. Rev. D **90** (2014) 054019.
- [74] Q. Chang, X. H. Hu, J. F. Sun, and Y. L. Yang, Phys. Rev. D **91** (2015) 074026.
- [75] J. F. Sun, Q. Chang, X. H. Hu, and Y. L. Yang, Phys. Lett. B **743** (2015) 444.
- [76] Q. Chang, J. F. Sun, Y. L. Yang, and X. N. Li, Phys. Lett. B **740** (2015) 56.
- [77] P. A. Zyla *et al.* [Particle Data Group], PTEP **2020** (2020) no.8, 083C01.
- [78] M. V. Terentev, Yad. Fiz. **24** (1976) 207 [Sov. J. Nucl. Phys. **24** (1976) 106].
- [79] V. B. Berestetsky and M. V. Terentev, Yad. Fiz. **25** (1977) 653 [Sov. J. Nucl. Phys. **25** (1977) 347].
- [80] W. Jaus, Phys. Rev. D **41** (1990) 3394.
- [81] W. Jaus and D. Wyler, Phys. Rev. D **41** (1990) 3405.
- [82] W. Jaus, Phys. Rev. D **60** (1999) 054026.
- [83] W. Jaus, Phys. Rev. D **67** (2003) 094010.
- [84] H. M. Choi and C. R. Ji, Phys. Rev. D **89** (2014) no. 3, 033011.
- [85] Q. Chang, L. T. Wang and X. N. Li, JHEP **1912** (2019) 102.

- [86] Q. Chang, X. N. Li, X. Q. Li, F. Su and Y. D. Yang, Phys. Rev. D **98** (2018) no.11, 114018.
- [87] H. M. Choi, H. Y. Ryu and C. R. Ji, Phys. Rev. D **96** (2017) no.5, 056008.
- [88] H. M. Choi, [arXiv:2108.10544 [hep-ph]].
- [89] H. M. Choi, arXiv:2102.02015 [hep-ph].
- [90] Q. Chang, X. N. Li and L. T. Wang, Eur. Phys. J. C **79** (2019) no.5, 422.
- [91] H. M. Choi and C. R. Ji, Phys. Rev. D **102** (2020) no.3, 036005.
- [92] Q. Chang, X. L. Wang and L. T. Wang, Chin. Phys. C **44** (2020) no.8, 083105.
- [93] H. M. Choi and C. R. Ji, Phys. Rev. D **95** (2017) no.5, 056002.
- [94] H. M. Choi and C. R. Ji, Phys. Rev. D **91** (2015) no.1, 014018.
- [95] C. W. Hwang and R. S. Guo, Phys. Rev. D **82** (2010) 034021.
- [96] D. S. Du, J. W. Li and M. Z. Yang, Phys. Lett. B **619** (2005) 105.
- [97] M. Z. Yang, Mod. Phys. Lett. A **21** (2006) 1625-1628.
- [98] K. Maltman, Phys. Lett. B **462** (1999) 14.
- [99] P. Ball and R. Zwicky, Phys. Rev. D **71** (2005) 014015.
- [100] P. Ball and R. Zwicky, Phys. Rev. D **71** (2005) 014029.
- [101] C. D. Lu, W. Wang and Z. T. Wei, Phys. Rev. D **76** (2007) 014013.
- [102] R. C. Verma, J. Phys. G **39** (2012) 025005.
- [103] W. F. Wang and Z. J. Xiao, Phys. Rev. D **86** (2012) 114025.
- [104] R. H. Li, C. D. Lu and W. Wang, Phys. Rev. D **79** (2009) 034014.
- [105] N. R. Soni, A. Issadykov, A. N. Gadaria, J. J. Patel and J. N. Pandya, [arXiv:2008.07202 [hep-ph]].

- [106] G. S. Bali *et al.* [RQCD], JHEP **08** (2019) 065.
- [107] P. Ball, V. M. Braun and A. Lenz, JHEP **05** (2006) 004.
- [108] H. M. Choi and C. R. Ji, Phys. Rev. D **75** (2007) 034019.
- [109] P. Ball and G. W. Jones, JHEP **03** (2007) 069.
- [110] A. Bharucha, D. M. Straub and R. Zwicky, JHEP **08** (2016) 098.
- [111] Q. Chang, S. J. Brodsky and X. Q. Li, Phys. Rev. D **95** (2017) no.9, 094025.
- [112] C. Wang, M. Z. Zhou and H. Chen, Eur. Phys. J. C **77** (2017) no.4, 219.
- [113] C. Wang, J. K. He and M. Z. Zhou, Eur. Phys. J. C **79** (2019) no.9, 765.
- [114] S. Uehara *et al.* [Belle], Eur. Phys. J. C **53** (2008) 1-14.
- [115] Y. S. Amhis *et al.* [HFLAV Collaboration], Eur. Phys. J. C **81** (2021) no.3, 226.
- [116] W. F. Wang, J. Chai and A. J. Ma, JHEP **03** (2020) 162.
- [117] Y. L. Shen, W. Wang, J. Zhu, C. D. Lu, Eur. Phys. J. C **50** (2007) 877.
- [118] C. S. Kim, Y. Li and W. Wang, Phys. Rev. D **81** (2010) 074014.
- [119] M. Beneke, T. Huber and X. Q. Li, Nucl. Phys. B **832** (2010) 109-151.
- [120] G. Bell, M. Beneke, T. Huber and X. Q. Li, Phys. Lett. B **750** (2015) 348-355.
- [121] G. Bell, M. Beneke, T. Huber and X. Q. Li, JHEP **04** (2020) 055.
- [122] T. Huber, S. Kränkl and X. Q. Li, JHEP **09** (2016) 112.
- [123] G. Bell, Nucl. Phys. B **795** (2008) 1-26.
- [124] G. Bell, Nucl. Phys. B **822** (2009) 172-200.
- [125] M. Beneke and S. Jager, Nucl. Phys. B **751** (2006) 160-185.
- [126] N. Kivel, JHEP **05** (2007) 019.

- [127] V. Pilipp, Nucl. Phys. B **794** (2008) 154-188.
- [128] M. Beneke and S. Jager, Nucl. Phys. B **768** (2007) 51-84.
- [129] C. S. Kim and Y. W. Yoon, JHEP **11** (2011) 003.